AMERICAN MUSEUM NOVITATES

Number 3694 August 23, 2010

Anatomy and Relationships of *Gilmoreosaurus mongoliensis* (Dinosauria: Hadrosauroidea) from the Late Cretaceous of Central Asia

ALBERT PRIETO-MÁRQUEZ[1] AND MARK A. NORELL[2]

ABSTRACT

The osteology of the hadrosauroid dinosaur *Gilmoreosaurus mongoliensis* is redescribed in detail based on the disarticulated cranial and postcranial elements of at least four individuals. These together constitute the lectotype and hypodigm of this species. The diagnosis is emended to include two autapomorphies (paddle-shaped postacetabular process that is less than 70% of the length of the iliac central plate and manual phalanx III-1 with greatly asymmetrical distal surface) and the unique combination of two iliac characters (presence of ischial tuberosity and supraacetabular process with apex located posterodorsal to ischial peduncle). The distinction of *G. mongoliensis* from *B. johnsoni* is confirmed on the basis of characters of the maxilla, dentition, ilium, ischium, and pubis. Maximum parsimony analysis places *G. mongoliensis* as a closely related outgroup to the Hadrosauridae, the sister taxon to the clade composed of all hadrosauroids closer to *Telmatosaurus transsylvanicus* than to *Bactrosaurus johnsoni*.

INTRODUCTION

Hadrosauroids are a diverse clade of ornithopod dinosaurs, consisting of *Hadrosaurus foulkii* Leidy, 1858, and all taxa more closely related to it than to *Iguanodon bernissartensis* Boulenger in Beneden, 1881 (Prieto-Márquez, 2010). These herbivores were equipped with

[1] Division of Paleontology, American Museum of Natural History (aprieto-marquez@amnh.org).
[2] Division of Paleontology, American Museum of Natural History (norell@amnh.org).

 ISSN 0003-0082

dental batteries with masticatory capability and, in the case of the most derived Late Cretaceous hadrosaurids, with hypertrophied nasal passages and elaborated supracranial ornamentation (Horner et al., 2004). The hadrosauroid fossil record is very rich and often well preserved, spanning the last 60 million years of the Cretaceous (Early Aptian to Late Maastrichtian) of Europe, Asia, the Americas, and Antarctica (Norman, 2002; You et al., 2003a; Lund and Gates, 2006).

Since the early 20th century, Asia has been the focus of numerous discoveries of hadrosauroid ornithopods that have filled a gap in our understanding of the early evolution of the clade, particularly regarding the skeletal modifications that took place from basal iguanodontians to hadrosaurids (Gilmore, 1933; Rozhdestvensky, 1966; Xu et al., 2000; Wang and Xu, 2001; You et al., 2003a, 2003b; Godefroit et al., 2005). One of the first hadrosauroids found in Asia, albeit one of most poorly understood, is *Gilmoreosaurus mongoliensis* (Gilmore, 1933; Brett-Surman, 1979).

The first fossil remains of *Gilmoreosaurus mongoliensis* were collected in 1923 by George Olsen during the Central Asiatic Expeditions of the American Museum of Natural History (Gilmore, 1933). The material consisted of disarticulated bones from various individuals from two quarries (AMNH localities 145 and 149) in the Upper Cretaceous Iren Dabasu Formation, Inner Mongolia, northern China (Godefroit et al., 1998).

The Iren Dabasu Formation (Berkey and Morris, 1922; Granger and Berkey, 1922) has yielded a diverse fauna that includes rays and sharks, plesiosaurs, turtles, lizards, crocodilians, pterosaurs, and theropod (dromaeosaurid, ornithomimid, troodontid, tyrannosaurid, therizinosaur), sauropod, ankylosaur, and ornithopod (hadrosauroid) dinosaurs, as well as various invertebrate groups (Currie and Eberth, 1993). Gilmore (1933) tentatively referred the fossils bones from localities 145 and 149 to the genus *Mandchurosaurus* (Riabinin, 1930) as the new species *M. mongoliensis.* This referral was motivated by a lack of characters distinguishing *M. mongoliensis* from *M. amurensis* at a generic level. However, no formal diagnosis of *M. mongoliensis* was provided; Gilmore noted only that there were "inconsistencies" between these two species.

Considering *Mandchurosaurus* as a nomen dubium, Brett-Surman (1975; 1979) removed Gilmore's hadrosaurid from that taxon and placed it in a new genus *Gilmoreosaurus* as the new combination *G. mongoliensis.* Furthermore, he provided the first diagnosis of *G. mongoliensis* in his master's thesis (Brett-Surman, 1975; see discussion below), which consisted of a combination of basal iguanodontian and hadrosaurid characters.

The taxonomic status and phylogenetic affinities of *Gilmoreosaurus mongoliensis* remains poorly understood. Originally, Gilmore (1933) recognized *Bactrosaurus johnsoni,* another hadrosauroid discovered in the same Iren Dabasu strata just about a kilometer from quarries 145 and 149, as distinct from *G. mongoliensis.* Gilmore primarily based his distinction on various osteological differences between the cranial and appendicular bones of these species. Although this distinction has been followed by several authors (Brett-Surman, 1975, 1979, 1989; Maryanska and Osmolska, 1981; Weishampel and Horner, 1986, 1990; Godefroit et al., 1998; Horner et al., 2004), other studies have synonymized *G. mongoliensis* with *B. johnsoni* (Rozhdestvensky, 1966; 1977).

The evolutionary relationship of *Gilmoreosaurus mongoliensis* within the Hadrosauroidea has remained contentious. While many studies have positioned this species within the Hadrosauridae (Gilmore, 1933; Young, 1958; Steel, 1969; Rozhdestvensky, 1966, 1977; Brett-Surman,

1975, 1979, 1989; Maryanska and Osmolska, 1981; Weishampel and Horner, 1986, 1990; Head, 1998; Kirkland, 1998), others have proposed a more basal phylogenetic placement as an outgroup taxon to hadrosaurids (Godefroit et al., 1998; Wagner, 2001; Prieto-Márquez et al., 2006b). Among those who considered *G. mongoliensis* a hadrosaurid, a number of authors (Gilmore, 1933; Brett-Surman, 1979; Maryanska and Osmolska, 1981; Weishampel and Horner, 1986) regarded it as a member of Hadrosaurinae, whereas others consider it a basal species outside the major radiation composed of Lambeosaurinae and Hadrosaurinae (Weishampel and Horner, 1990; Head, 1998; Kirkland, 1998; Horner et al., 2004).

This lack of consensus on the systematic position of *Gilmoreosaurus mongoliensis* primarily stems from the poor documentation of its remains, which have received only cursory description (Gilmore, 1933). The inadequacy of the description has limited comparison with the numerous hadrosauroid taxa that have been erected and described over the last several decades. In turn, this shortcoming has made it difficult to interpret *G. mongoliensis* in the context of current phylogenetic analyses. Importantly, *G. mongoliensis* is one of the rare Asian hadrosauroids for which the postcranial skeleton is nearly completely preserved.

Because this taxon has been largely ignored, the cranial and postcranial anatomy of *Gilmoreosaurus mongoliensis* is thoroughly described in detail. The osteological observations resulting from this study allow a reassessment of its taxonomic status and an emended diagnosis. For the first time, the evolutionary relationships of *G. mongoliensis* are resolved by integrating this species into a phylogenetic analysis encompassing a large taxonomic sample of hadrosauroid taxa, which, not counting the subject of this study, includes 12 of the 15 non-hadrosaurid hadrosauroid genera and 21 of the 28 hadrosaurid genera known as of 2009 (valid genera after Prieto-Marquez, 2010).

MATERIALS AND METHODS

Osteological description and character coding of *Gilmoreosaurus mongoliensis* was based on reexamination of all the material available for this species. The comparative osteological data and character coding for most of the hadrosauroid taxa were also obtained from direct observation of specimens. Exceptions were *Aralosaurus tuberiferus, Jaxartosaurus aralensis, Eolambia caroljonesa, Penelopognathus weishampeli, Probactrosaurus gobiensis, Nanyangosaurus zhugeii,* and *Shungmiaosaurus gilmorei,* the anatomical data of which had to be obtained from the literature.

The phylogenetic position of *Gilmoreosaurus mongoliensis* was inferred via parsimony analysis using the character data set of Prieto-Márquez (2010). In addition to *G. mongoliensis,* the present analysis included 40 hadrosauroid species (28 Hadrosauridae and 12 non-hadrosaurid Hadrosauroidea), sufficient enough to provide a wide representation of the taxonomic diversity of the clade. Outgroup taxa consisted of two non-hadrosauroid iguanodontoidean species, *Iguanodon bernissartensis* and *Mantellisaurus atherfieldensis.* The character data of Prieto-Márquez (2010) consisted of 286 equally weighted morphological characters (196 cranial and 90 postcranial). Characters 1, 4, 16, and 19 were ordered, following the recommendation of Prieto-Márquez (2010). The search for the optimal tree(s) using maximum parsimony was

conducted in TNT version 1.0 (Goloboff et al., 2008). A heuristic search of 10,000 replicates using random additional sequences was performed, followed by branch swapping by tree-bisection-reconnection (TBR; Swofford et al., 1996) holding 10 trees per replicate. Bremer support (Bremer, 1988) was assessed by computing decay indices (Donoghue et al., 1992) using MacClade version 4.0 (Maddison and Maddison, 2003) and PAUP version 4.0b10 (Swofford, 2002). Bootstrap proportions (Felsenstein, 1985) were also calculated using PAUP, setting the analysis to 5,000 replicates using heuristic searches, where each search was conducted using random additional sequences with branch-swapping by subtree pruning and regrafting (SPR) and 25 replicates.

SYSTEMATIC PALEONTOLOGY

Dinosauria Owen, 1842
Ornithischia Seeley, 1888
Ornithopoda Marsh, 1881
Iguanodontia Dollo, 1888
Hadrosauroidea Cope, 1870
Gilmoreosaurus Brett-Surman, 1979

G. mongoliensis Gilmore, 1933

Lectotype: AMNH FARB 30735, a complete right ilium.

Referred Material: AMNH FARB 30653, right maxilla; AMNH FARB 30655, left lacrimal; AMNH FARB 30656, right lacrimal; AMNH FARB 30657, partial right jugal; AMNH FARB 30658, partial right squamosal; AMNH FARB 30659, left quadrate; AMNH FARB 30660, partial right quadrate; AMNH FARB 30654, partial right dentary; AMNH FARB 30661, dentary tooth; AMNH FARB 30662 through 30669, eight maxillary tooth crowns; AMNH FARB 30670, cervical vertebral centrum; AMNH FARB 30671–30673, three nearly complete middle-posterior cervical vertebrae; AMNH FARB 30674 and 30675, two anterior dorsal centra; AMNH FARB 30676 and 30677, two anterior dorsal neural arches with diapophyses and neural spines; AMNH FARB 30678, 30679, and 30680, three nearly complete vertebrae; AMNH FARB 30681 and 30682, two partial middle dorsal vertebrae; AMNH FARB 30683–30685, three partial posterior dorsal vertebrae; AMNH FARB 30686, four fused sacral neural arches with neural spines; AMNH FARB 30687, four coossified sacral centra; AMNH FARB 30688, three coossified sacral centra with partial transverse processes and neural arches; AMNH FARB 30689 through 30695, seven proximal caudal vertebrae; AMNH FARB 30696 through 30721, 26 distal caudal vertebrae; AMNH FARB 30722, 30723, and 30724, three left coracoids; AMNH FARB 30725, left scapula; AMNH FARB 30726 and 30727, two right scapulae; AMNH FARB 30728, right humerus; AMNH FARB 30729, left ulna and left radius; AMNH FARB 30730, left metacarpal IV; AMNH FARB 30731, right metacarpal IV; AMNH FARB 30732, right manual phalanx II-1; AMNH FARB 30733, right manual phalanx III-1; AMNH FARB 30734, partial left ilium; AMNH FARB 30735 and 30736, two right ilia; AMNH FARB 30737, preacetabular process of left ilium; AMNH FARB 30738, partial right pubis; AMNH FARB 30739, left ischium;

AMNH FARB 30740, right ischium; AMNH FARB 30741, right femur; AMNH FARB 30742–30745, four left tibiae; AMNH FARB 30746 and 30747, two right tibiae; AMNH FARB 30748 and 30749, two left fibulae; AMNH FARB 30750 a left astragalus; AMNH FARB 30751 and 30752, two right astragali; AMNH FARB 30753, right calcaneum; AMNH FARB 30754 and 30755, two right metatarsals III; AMNH FARB 30756 and 30757, two right metatarsals IV; AMNH FARB 30758, left pedal phalanx II-1; AMNH FARB 30759 and 30760, two right pedal phalanges II-1; AMNH FARB 30765, left pedal phalanx II-2; AMNH FARB 30761, right pedal phalanx III-1; AMNH FARB 30762, left pedal phalanx III-1; AMNH FARB 30763, left pedal phalanx IV-1; AMNH FARB 30764, right pedal phalanx IV-1; AMNH FARB 30766, right distal pedal phalanx from digit IV; AMNH FARB 30767, left distal pedal phalanx from digit IV; AMNH FARB 30768–30773, six ungual phalanges; and AMNH 6369, a nearly complete predentary (Gilmore [1933] originally listed this specimen as cotype of *Gilmoreosaurus mongoliensis*; however, because the International Code of Zoological Nomenclature currently does not contemplate cotypes [International Commission on Zoological Nomenclature, 1999], this specimen is here included in the hypodigm). All these bones, including the lectotype ilium, represent a minimum number of four individuals, based on the maximum number of bones from the same side of the most abundant element in the sample, the tibia.

Except AMNH FARB 6369, all the elements were originally cataloged as a single lot as AMNH FARB 6551. Current cataloguing practices do not provide for lot cataloging of separate individuals. Therefore, we have recataloged the individual elements as separate numbers and designated AMNH FARB 30735, a complete right ilium, the lectotype specimen. The only evidence for association of more than one bone to a single specimen was found in the only left radius and ulna; these two elements match in size and articulate with each other in such a way that it is likely that they correspond to the same individual.

Occurrence: Approximately 14 km east of the Iren Dabasu telegraph station (Gilmore, 1933) and 14 km northeast of the town of Erenhot, Inner Mongolia (northern China), near the border with Mongolia (Young, 1958; Godefroit et al., 1998). The two quarries (AMNH localities 145 and 149) where the bones were collected are located approximately 1 km apart from one other (Godefroit et al., 1998) and lie in the Iren Dabasu Formation. Considerable debate has surrounded the age of this formation: it has been estimated as Early Cretaceous (Berkey and Morris, 1927), Cenomanian (Rozhdestvensky, 1966; 1977), pre-Turonian (Weishampel and Horner, 1986), pre-Santonian (Brett-Surman, 1979), Early Late Creatceous (Godefroit et al., 1998), Early Campanian (Jerzykiewicz and Russell, 1991; Currie and Eberth, 1993), and Maastrichtian (Chen, 1983; Liu and Wu, 1990). More recently, Van Itterbeeck et al. (2005) restudied the stratigraphy and sedimentology of the Iren Dabasu Formation and concluded that it is most probably latest Campanian–Early Maastrichtian in age. They base this conclusion on the age provided by microfossils, particularly four species of charophytes and eight species of ostracods.

Emended Diagnosis: Hadrosauroid ornithopod characterized by the following autapomorphies and unique combination of characters: paddle-shaped postacetabular process that is less then 70% of the length of the iliac central plate; ilium combining the presence of ischial tuberosity and supraacetabular process with apex located posterodorsal to ischial peduncle; manual phalanx III-1 with greatly asymmetrical distal surface.

OSTEOLOGY

Cranial Elements

Maxilla: The maxilla of *Gilmoreosaurus mongoliensis* (AMNH FARB 30653) is triangular in lateral view and dorsoventrally shallow, being three times longer than it is tall at midlength (fig. 1). At the anterior end of the element, the anteroventral process is missing adjacent to the large rostral foramen. This foramen is elliptical, opening anterolaterally and slightly dorsally (fig. 1A–B). Its relatively low position within the ventral half of the anterodorsal region of the maxilla, just posterior to the anteroventral process of the maxilla, is typical of non-hadrosaurid hadrosauroids such as *Equijubus normani* (IVPP V12534) and *Jinzhousaurus yangi* (IVPP V12691). This is in contrast with the condition in hadrosaurids, where the large rostral maxillary formen occupies a much higher position within the dorsal half of the anterodorsal region of the maxilla (e.g., *Gryposaurus notabilis,* ROM 873, or *Lambeosaurus lambei,* CMN 351).

Medial to the rostral foramen is the anterodorsal process of the maxilla, which is present in all iguanodontoideans except Lambeosaurinae (Horner et al., 2004). The process is medially offset from the anterior body of the maxilla and projects anteroventrally, its dorsal margin forming a 20° angle to the tooth row (fig. 1B). The lateral surface of the process is nearly vertical (showing a slight dorsal orientation) and supported the posteroventral process of the premaxilla. This articular surface becomes dorsoventrally wide toward the anteroventral end of the maxilla. Posteriorly, this surface becomes continuous with a narrow premaxillary groove that extends until the lacrimal contact with the maxilla, parallel with the anterodorsal margin of the element (fig. 1B). The medial side of the anterodorsal process has a large longitudinal ridge. This ridge extends medially and slightly dorsally, and forms the medial margin of a wide and shallow groove (fig. 1A, C). The lateral margin of this groove is formed by the dorsal margin of the anterodorsal process. The groove represents the articular facet for the anterior end of the vomer. Below the medial ridge lies the anterior region of the dental parapet in the medial wall of the maxilla.

The anterodorsal region of the lateral surface of the maxilla is shallow, as in non-hadrosaurid hadrosauroids such as *Telmatosaurus transsylvanicus* (e.g., NHM R3386). In contrast, all hadrosaurids except *Brachylophosaurus canadensis* (e.g., MOR 1071-7-6-98-79) and *Maiasaura peeblesorum* (OTM F138) show a more elevated anterodorsal region of the maxilla than their hadrosauroid outgroup taxa (Prieto-Márquez, 2010).

In *Gilmoreosaurus mongoliensis,* as in non-hadrosaurid hadrosauroids such as *Bactrosaurus johnsoni* and *Telmatosaurus transsylvanicus* (Prieto-Márquez and Wagner, 2009), the articular facet for the jugal perches above the ectopterygoid ridge, lying on a promontorium that is elevated and detached from the anterior ectopterygoid shelf (fig. 1B). On this promontorium the articular surface slopes ventrally to face laterodorsally. A thick ridge limits the posterior extent of the jugal's articular facet, where the promontorium protrudes posterolaterally forming the apex of the jugal process (fig. 1B). A row of three peribuccal foramina lay below the lateral margin of the jugal process, near the anterior limit of the ectopterygoid shelf. Dorsal to the promontorium, on the lateral surface of the base of the dorsal process of the maxilla, the jugal-maxilla joint surface faces laterally and wedges anteriorly into a sharp point. This

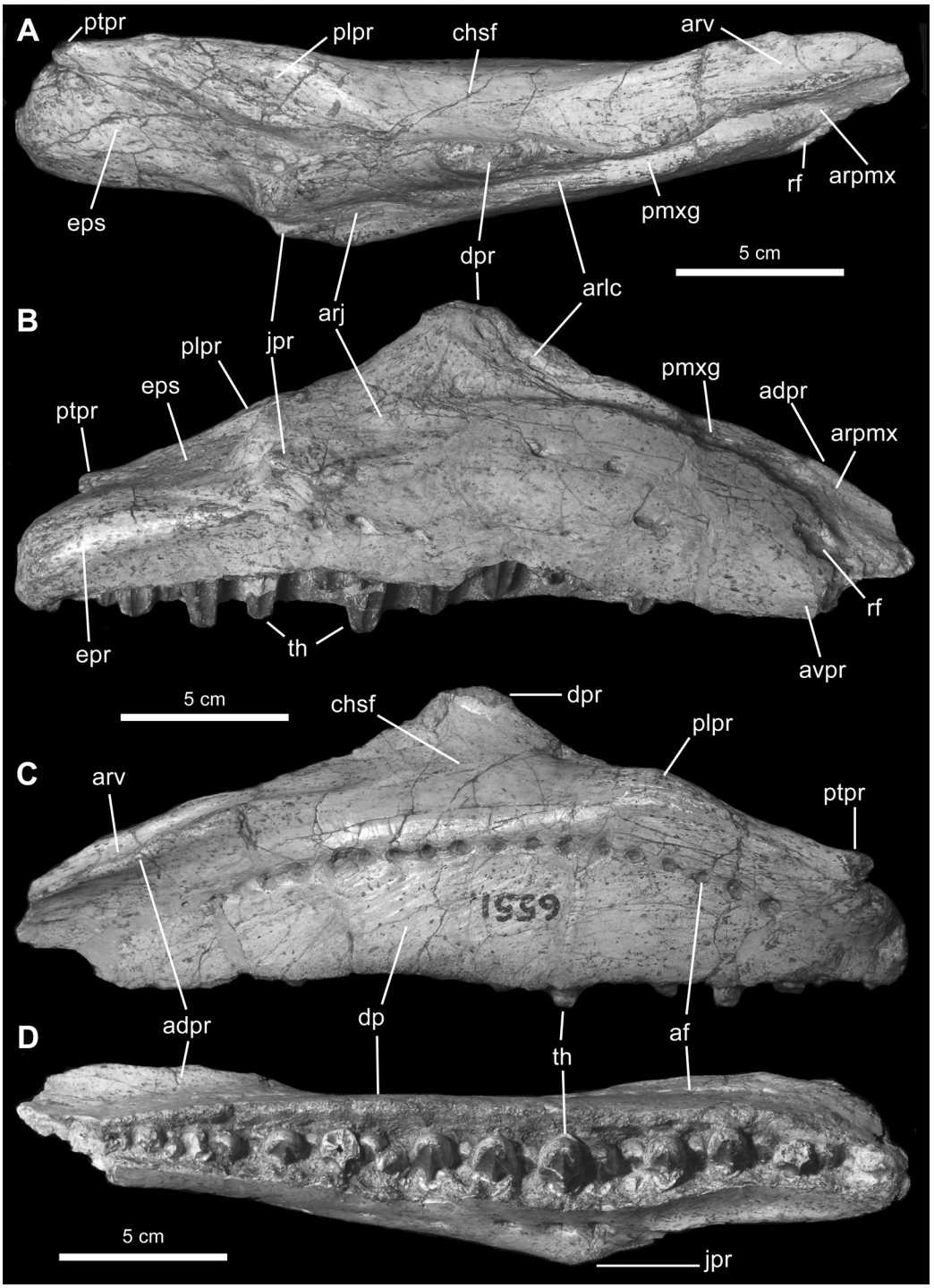

FIGURE 1. Right maxilla of *Gilmoreosaurus mongoliensis* (AMNH FARB 30653). **A,** dorsal; **B,** lateral; **C,** medial; **D,** ventral. Abbreviations in appendix 2.

suggests that the anterior end of the rostral process of the jugal was pointed. The dorsal region of the jugal-maxilla joint is separated by an anteroventrally directed ridge from the articular surface for the lacrimal. The latter facet is dorsoventrally narrow and occupies the anterodorsal region of the preserved lateral surface of the dorsal process of the maxilla. The dorsal maxillary process is low, triangular, and mediolaterally compressed. Its anterior and posterior margins form an angle of approximately 110°. The base of the dorsal process is centered relative to the anteroposterior length of the maxilla. The posterior margin of the process slopes posteroventrally in continuity with the posteromedial border of the promontorium holding the jugal-maxilla joint.

The posterior third of the maxilla contains the palatine and pterygoid processes medially and the ectopterygoid shelf and ridge laterally. Posteroventral to the jugal process, the ectopterygoid ridge is proximally narrow but abruptly thickens and forms slightly more than the dorsal half of the depth of the lateral surface of the maxilla. The ectopterygoid shelf is mediolaterally wide and slopes posteroventrally to form an angle of 19° to the posterior segment of the tooth row. This condition is shared with the hadrosauroid *Telmatosaurus transsylvanicus* and the hadrosaurid *Secernosaurus koerneri,* and is in contrast with the more pronounced slopes of other hadrosauroids and the nearly horizontal shelves of hadrosaurids (Prieto-Márquez, 2008: fig. D56). In *Gilmoreosaurus mongoliensis* the ectopterygoid shelf accounts for 30% of the total length of the maxilla, as in non-hadrosaurid hadrosauroids such as *Bactrosaurus johnsoni* (e.g., AMNH FARB 6553) and *Protohadros byrdi* (SMU 74582).

The palatine process forms the dorsal margin of the posteromedial wall of the maxilla and the mediodorsal border of the ectopterygoid shelf. The process bulges smoothly from the dorsal profile of the maxilla, showing an anteriorly skewed medial contour. Posteroventrally, the palatine process slopes gently becoming continuous with the pterygoid process. The latter lies at the posteromedial corner of the maxilla and projects posteriorly a short distance. Its distal end is incompletely preserved. This process is mediolaterally compressed and separated from the ectopterygoid shelf by a short cleft.

The medial surface of the maxilla is flat and bounded by the parapet of the dental battery. A slightly arched row of alveolar foramina is located within the dorsal half of the maxilla. There are a minimum of 26 alveolar positions in the maxilla, the precise number being uncertain due to incomplete preservation of teeth and alveoli. Of these, 22 alveoli bear teeth at different stages of eruption. All but one of these teeth are still unworn. There is no trace of the longitudinal ventral vascular furrow that is commonly present in the maxillae of other hadrosauroids (e.g., *Bactrosaurus johnsoni,* AMNH FARB 6553, or *Brachylophosaurus canadensis,* MOR 1071-8-13-98-559).

Jugal: The only preserved jugal (AMNH FARB 30657) is missing the anteriormost region of the rostral process, the distal end of the postorbital ramus, and most of the posterior region above the posteroventral flange (fig. 2). The fragment is triradiate in lateral profile. The ascending postorbital ramus forms a 120° angle to the long axes of the rostral process and the posteroventral region of the jugal, whereas the latter forms an angle of 130° to the long axis of the rostral process. The jugal is mediolaterally compressed and anteroposteriorly arched, showing a concave medial side in dorsal and ventral views.

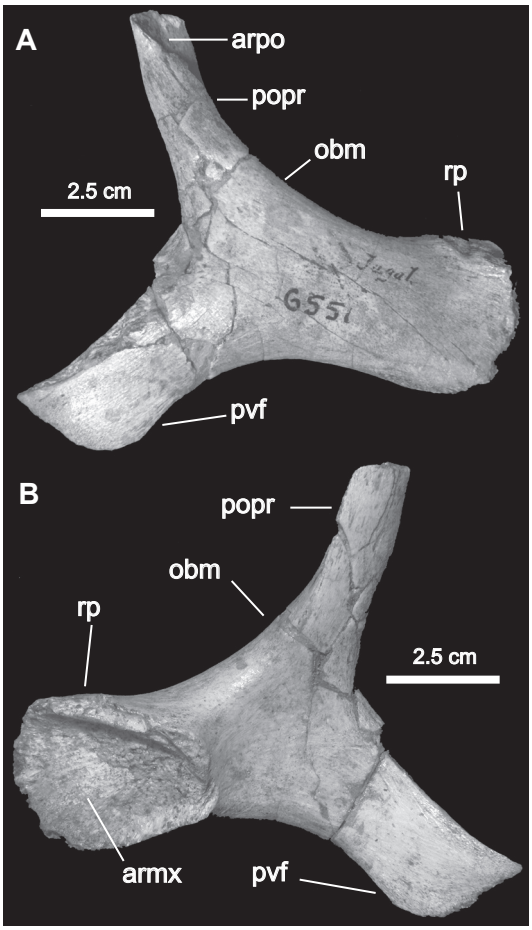

FIGURE 2. Right jugal of *Gilmoreosaurus mongoliensis* (AMNH FARB 30657). **A,** lateral; **B,** medial. Abbreviations in appendix 2.

As preserved, the rostral process is subrectangular in lateral and medial profiles, and slightly expanded dorsoventrally at its anterior end. The posterodorsal margin is dorsoventrally shallow, in contrast to the deeper region seen in the Hadrosauridae (Weishampel et al., 1993) and similar to the condition present in relatively basal hadrosauroids like *Equijubus normani* (IVPP V12534), *Jinzhousaurus yangi* (IVPP V12691), *Probactrosaurus gobiensis* (Norman, 2002), or *Lophorhothon atopus* (FMNH P27383). The lateral surface of the rostral process is gently concave, while its medial side contains the articular surface for the maxilla. This surface extends over the entire length and depth of the rostral process, facing medially and slightly ventrally. It is strongly concave posterodorsally and bounded by a prominent rim of bone dorsally, posteriorly, and posteroventrally. This bony rim is thick dorsally and posteriorly. The orientation and morphology of this articular surface in *Gilmoreosaurus mongoliensis* is similar to that seen in non-hadrosaurid hadrosauroids, such as *Tanius sinensis* (e.g., PMU R240), *Protohadros byrdi* (SMU 74582), and *Bactrosaurus johnsoni* (e.g., AMNH FARB 6373). The articular surface shows numerous faint striations that radiate anterodorsally, anteriorly, and anteroventrally from its concave posterior terminus.

The proximodorsal surface of the rostral process forms a flat shelf that is posteriorly continuous with the base of the postorbital ramus. The latter projects dorsally, while being slightly tilted posteriorly. Both the dorsal surface of the proximal region of the rostral process and the anterior surface of the postorbital ramus form the anteroventral orbital margin. The proximal segment of the postorbital ramus is triangular in cross section due to the presence of anterior, lateral, and posteromedial surfaces. Distally, the anterior surface of the ramus is incised with a large triangular excavation that wedges ventrally to accommodate the distal end of the jugal ramus of the postorbital.

The preserved ventral region of the posteroventral flange of the jugal is D-shaped in lateral profile. The straight anteroventral and posteroventral margins of the flange lay at an angle of 105° from each other. Posteriorly, the flange becomes mediolaterally thinner.

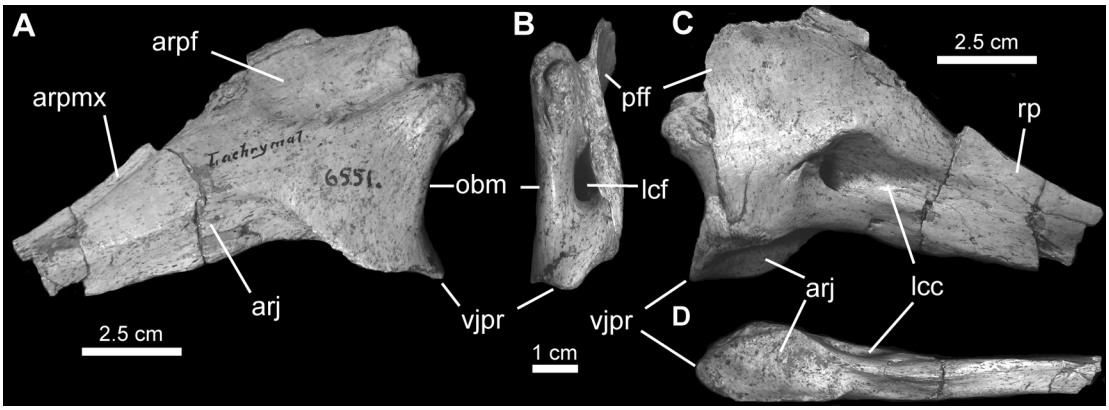

FIGURE 3. Left lacrimal of *Gilmoreosaurus mongoliensis* (AMNH FARB 30655). **A,** lateral; **B,** posterior; **C,** medial; **D,** ventral. Abbreviations in appendix 2.

Lacrimal: As is common in non-lambeosaurine hadrosauroids, the lacrimal (AMNH FARB 30655 and 30656) is wedge shaped in lateral view (fig. 3). This bone is mediolaterally compressed and contributes to the anterior margin of the orbit. The triangular rostral process projects anteroventrally. Its lateral surface is bounded by two medially recessed facets (fig. 3A). The dorsal facet is very narrow and overlapped by the ventral margin of the posteroventral process of the premaxilla. The ventral facet, which is overlapped by the dorsal margin of the rostral process of the jugal, is twice as wide as the dorsal facet and is bounded posteriorly by the ventral jugal. The posterodorsal region of the lacrimal shows an extensive recessed and smooth surface for reception of the anteroventral process of the prefrontal. The anteroventral, ventral, and posteroventral margins of this facet form an arcuate border, which probably mirrors the same contour of the anteroventral border of the prefrontal, as is typical in other hadrosauroids (e.g., *Brachylophosaurus canadensis,* MOR 794). Although incompletely preserved, the dorsal margin of the articular recess for the prefrontal rises dorsal to the posterodorsal corner of the lacrimal.

The ventral jugal process forms the posteroventral region of the lacrimal (fig. 3A), where the element reaches its greatest mediolateral width. The process is subtriangular in lateral view. The ventral surface forms a subelliptical and deep excavation for reception of the posterodorsal corner of the rostral process of the jugal (fig. 3D). The lateral margin of the jugal process describes a convex ventral profile and is ventrally offset relative to the medial margin (fig. 3C).

The posterolateral orbital margin of the lacrimal is gently concave in lateral profile and is continuous ventrally with the ventral jugal process. The posterior orbital surface of the lacrimal is pierced by a mediolaterally compressed and dorsoventrally elongate foramen (fig. 3B). This lacrimal foramen communicates internally with the lacrimal canal, which exits through a large circular foramen on the ventral surface ventrally (fig. 3C). The medial circular foramen of the lacrimal canal is anteriorly continuous with a wedge-shaped excavation, which progressively shallows anteriorly until disappearing into the slightly convex medial surface of the anterior terminus of the lacrimal. Dorsal to the lacrimal canal, the medial surface of the prefrontal flange is smooth and slightly concave dorsoventrally, as the flange gently curves medially (fig. 3C).

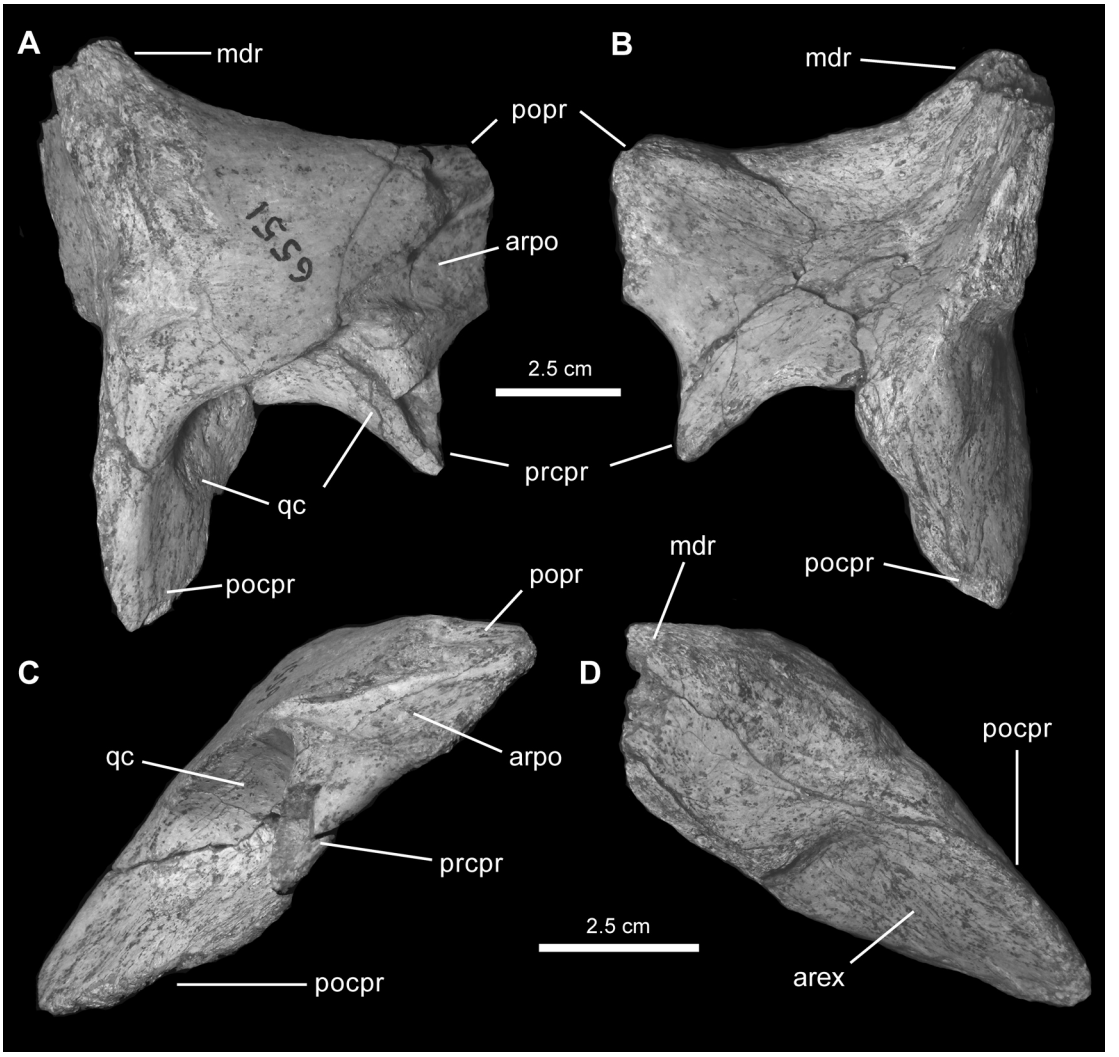

FIGURE 4. Right squamosal of *Gilmoreosaurus mongoliensis* (AMNH FARB 30658). **A,** dorsolateral; **B,** ventromedial; **C,** anterior; **D,** posteroventral. Abbreviations in appendix 2.

Squamosal: The central body of the squamosal (AMNH FARB 30658) is subtriangular in laterodorsal view and its external surface is very slightly convex (fig. 4). In contrast, its ventromedial surface is deeply concave and is bisected by a low and poorly defined ridge. Three major features project from the central body of the squamosal: the postorbital process anteriorly, the postcotyloid process lateroventrally, and the medial ramus. Only the proximal region of the postorbital process is preserved. It is mediodorsally compressed so that dorsal and ventral margins are nearly parallel. The dorsolateral surface contains a triangular excavation for reception of the posterior ramus of the postorbital. This articular excavation occupies the ventral half of the dorsolateral surface of the postorbital process, with the posteroventral apex of its triangular outline lying adjacent to the quadrate cotylus.

The quadrate cotylus is twice as wide as it is dorsoventrally high and it has a straight dorsal margin. The cotylus is bounded anteriorly by the precotyloid process and posteriorly by the postcotyloid process (fig. 4A). The precotyloid process is triangular and relatively short, only slightly longer than half the width of the quadrate cotylus. There is no precotyloid fossa (Gates and Sampson, 2007: fig. 7). Among non-hadrosaurid hadrosauroids the fossa is also absent in *Bactrosaurus johnsoni* (e.g., AMNH FARB 6365) and *Tanius sinensis* (PMU R240), being faintly developed in *Lophorhothon atopus* (FMNH P27383), and present in *Equijubus normani* (IVPP V12534) and *Jinzhousaurus yangi* (IVPP V12691). The distribution of this feature is also variable within the Hadrosauridae, being present in most taxa except *Jaxartosaurus aralensis* (PIN 1/5009), *Charonosaurus jiayinensis* (CUST JV1251-57) and the three species of *Parasaurolophus* (e.g., ROM 768, NMMNH P-25100, and UCMP 143270).

The postcotyloid process is bullet shaped in posteroventral and anterodorsal views (fig. 4C–D). The process is compressed along a posteroventral to anterodorsal axis. This compression is more obvious distally. Its posteroventral surface is recessed relative to the posteromedial side of the squamosal. This recessed surface is overlapped by the proximal region of the paroccipital process of the exoccipital. Medial to the posteroventral surface of the postcotyloid process, the ventral margin of the posteromedial region of the squamosal is incompletely preserved, lacking the articular facet for the supraoccipital. The posteromedial surface of the squamosal shows a different, more vertical orientation in contrast to the posteroventral face of the postcotyloid process, forming a 90° angle with the dorsolateral surface of the central region of the bone. Only the proximalmost region of the medial ramus of the squamosal is preserved.

Quadrate: The quadrate (AMNH FARB 30659 and 30660) is nearly straight, showing only very gentle curvature along its posterior margin (fig. 5A). The articular surface of the quadrate head is triangular and mediolaterally compressed (fig. 5B). A well-developed squamosal buttress lies along the dorsal segment of the posterior margin of the quadrate, adjacent to the articular head (fig. 5A). The buttress is relatively long, extending only 25% of the length of the quadrate. This feature is typically present in basal iguanodontians and non-hadrosaurid hadrosauroids, as well as in a few hadrosaurids such as *Brachylophosaurus canadensis* and *Gryposaurus notabilis* (Prieto-Márquez, 2010).

The lateral surface of the quadrate is flat and the anterior margin bears a wide quadratojugal notch (fig. 5A). The center of the notch is located ventral to the midlength of the quadrate, as in many (but not all) hadrosauroids (*Bactrosaurus johnsoni, Protohadros byrdi, Tanius sinensis, Lophorhothon atopus, Telmatosaurus transsylvanicus*), and hadrosaurine hadrosaurids (Prieto-Márquez, 2010). Most of the articular margin of the notch is missing, except for a narrow dorsal portion and an elongate ventral facet. The latter projects anterolaterally and is elliptical and is located on a protuberance (fig. 5A). However, the prominence of this protuberance is most likely an artifact of missing bone on the articular quadratojugal margin immediately dorsal to the facet. Although incomplete, enough of the lateral profile of the quadratojugal notch is preserved to demonstrate that it is asymmetrical, with a longer dorsal margin, as in *Bactrosaurus johnsoni, Lophorhothon atopus,* and a few hadrosaurids such as *Prosaurolophus maximus* and *Saurolophus* spp. (Prieto-Márquez, 2010).

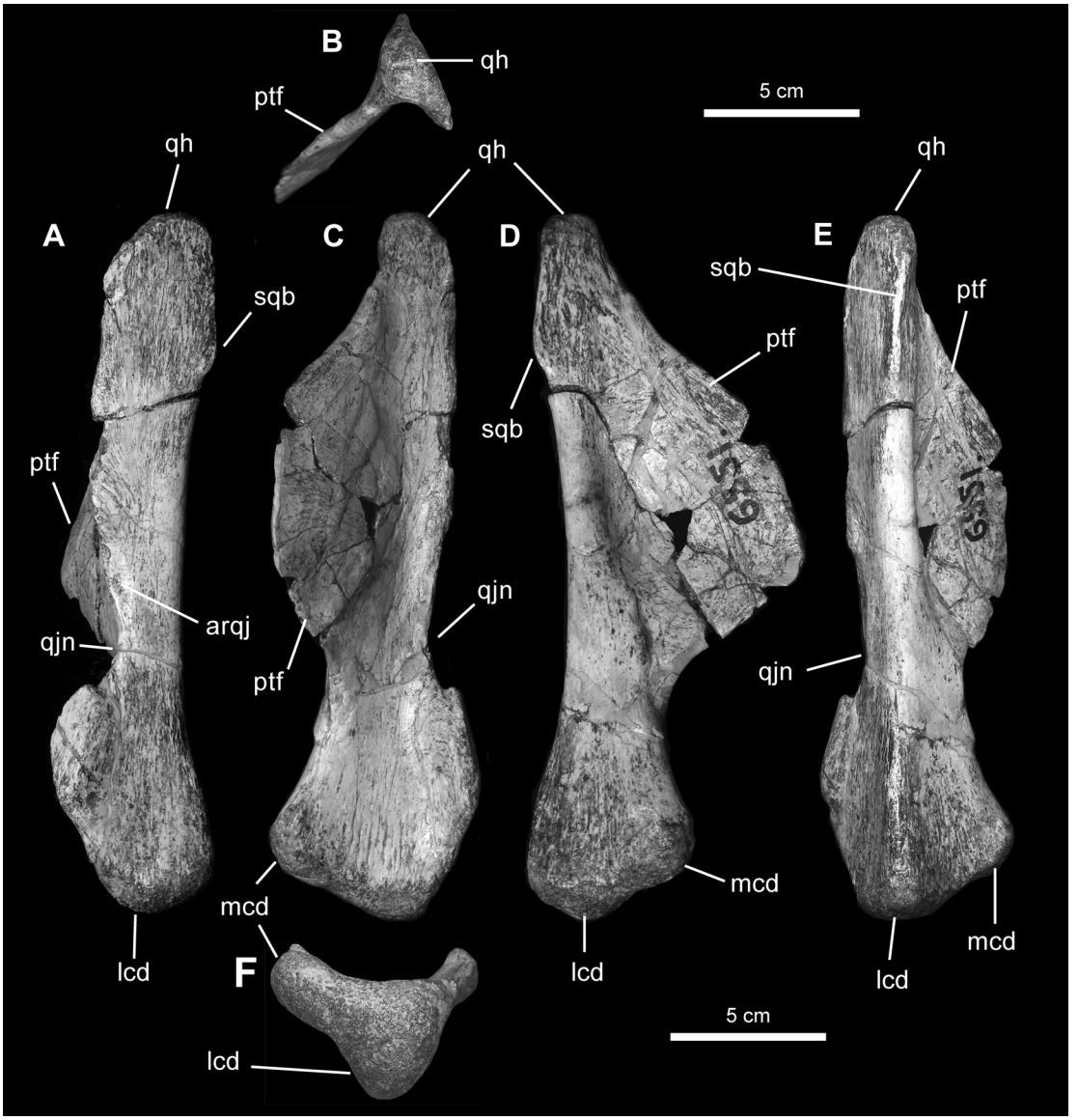

FIGURE 5. Left quadrate of *Gilmoreosaurus mongoliensis* (AMNH FARB 30659). **A,** lateral; **B,** dorsal; **C,** anterior; **D,** medial; **E,** posterior; **F,** ventral. Abbreviations in appendix 2.

The jugal flange, which typically extends anteriorly above the quadratojugal notch, is not preserved. However, the pterygoid flange is nearly complete (fig. 5C–D), being a triangular lamina that projects anteromedially from the medial margin of the quadrate. Dorsally, it originates near the articular head, and dorsoventrally 75% of the length of the quadrate. The ventral terminus of the flange merges with the anteromedial margin of the quadrate at a level just above the ventral facet of the quadratojugal notch. Most of the medial surface of the pterygoid flange is occupied by a deep fossa, while the lateral side is dorsoventrally convex (fig. 5C). The anterome-

dial margin of the pterygoid flange is thin, slightly thickening dorsally toward the quadrate head.

Ventrally, the quadrate is mediolaterally expanded (fig. 5C) and contains two condyles, which form a skewed triangular distal profile (fig. 5F). The larger lateral condyle articulates with the surangular and displays an equilateral triangular cross section. In contrast, the medial condyle, which articulates with the articular one, is mediolaterally elongate and subrectangular in cross section. This configuration is similar to that in basal iguanodontians and most non-hadrosaurid hadrosauroids except *Telmatosaurus transsylvanicus* and *Lophorhothon atopus* (Prieto-Márquez, 2010). In the latter two and in the Hadrosauridae, the difference in size between the lateral and medial condyle is greater (Horner et al., 2004; Prieto-Márquez, 2008). Likewise, in the quadrate of *G. mongoliensis* the ventral offset of the lateral condyle relative to the articular margin of the medial condyle is less developed than in the Hadrosauridae, but similar to that observable in non-hadrosaurid hadrosauroids such as *Bactrosaurus johnsoni, Equijubus normani,* or *Protohadros byrdi* (Prieto-Márquez, 2010).

Predentary: The predentary (AMNH FARB 6369) is a U-shaped mediolaterally elongate bar from which two long processes project posterolaterally (fig. 6). The corners of the predentary describe smooth curved profiles in dorsal and ventral views. The maximum mediolateral width of the predentary is approximately equal to the length of the lateral processes, as in non-hadrosaurid hadrosauroids such as *Bactrosaurus johnsoni* (e.g., SBDE 95E5/36, Godefroit et al., 1998) and *Protohadros byrdi* (SMU 74582), and some hadrosaurids (Prieto-Márquez, 2008: fig. C1). The anterior surface of the predentary is nearly perpendicular, forming an 80° angle to the dorsal margin of each lateral process; this condition is present in hadrosauroid outgroup taxa such as

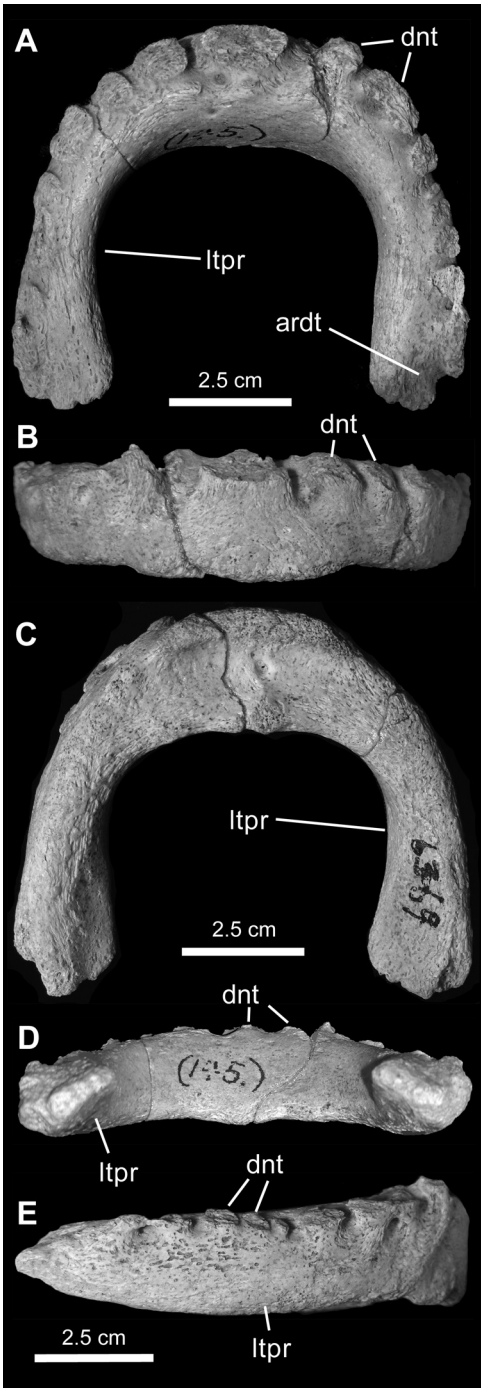

FIGURE 6. Predentary of *Gilmoreosaurus mongoliensis* (AMNH FARB 6369). **A,** dorsal; **B,** anterior; **C,** ventral; **D,** posterior; **E,** right lateral. Abbreviations in appendix 2.

Iguanodon bernissartensis (e.g., IRSNB 1534) and *Mantellisaurus atherfieldensis* (IRSNB 1551), and in some non-hadrosaurid hadrosauroids such as *Protohadros byrdi* (SMU 74582). The posterior surface of the predentary of *Gilmoreosaurus mongoliensis* is smooth, flat, and slightly anteriorly inclined. It lacks a ridge on the lingual surface. A nearly vertical keellike ridge lies on the posteroventral process of the predentary in hadrosaurids, but is absent in *Bactrosaurus johnsoni, Protohadros byrdi, Protohadros byrdi,* and more basal iguanodontians such as *Iguanodon bernissartensis* and *Mantellisaurus atherfieldensis* (Prieto-Márquez, 2010). A small median protuberance present on the ventral margin of the posterior surface of the predentary of *G. mongoliensis* may be the remnant of a ridgeless posteroventral process.

The ventral side of the anterior predentary bar contains a large and mediolaterally elongate depression, which is bounded by prominent edges of the ventral borders of the anterior and posterior surfaces. A small foramen is present at the center of this depression. The prominence of the ventral edge of the anterior face of the predentary is probably all that is left of the ventral median process.

The predentary denticles are not limited to the anterior oral margin, but extend posteriorly onto the lateral processes, as in basal iguanodontians (e.g., *Iguanodon* sp., NHM R105) and non-hadrosaurid hadrosauroids such as *Probactrosaurus gobiensis* (Norman, 2002) and *Equijubus normani* (IVPP V12534). All the denticles are eroded and truncated near their bases (fig. 6A). There are seven denticles on the dorsal surface of each lateral process, plus an additional larger denticle at the sagittal plane of the predentary. A few denticles are elongate and appear to be composed of the fusion of two denticles. Although the space between two consecutive denticles is smaller than the diameter of the base of each denticle, it is uncertain whether the spacing between complete denticles would be as reduced, a condition found in most hadrosaurids but not in their outgroup taxa (Prieto-Márquez et al., 2006b).

Each lateral process is slightly compressed mediolaterally along its proximal region becoming progressively more dorsoventrally compressed and mediolaterally expanded toward its distal end (fig. 6E). As in *Bactrosaurus johnsoni* (e.g., SBDE 95E5/36, Godefroit et al., 1998) and *Probactrosaurus gobiensis* (Norman, 2002), the predentary of *Gilmoreosaurus mongoliensis* has a shallow, short dentary shelf that is limited to the posterolateral region of each lateral process (fig. 6A).

Dentary: The only preserved dentary (AMNH FARB 30654) consists of most of the main ramus with a heavily eroded and edentulous dental battery (fig. 7). The dentary ramus is four times longer than it is high at midlength. Approximately 15 alveoli are present. As these alveoli cover most of the length of the dental battery of the specimen, it is likely that the total number of teeth in this taxon did not exceed 30, which is primitive for hadrosauroids (Horner et al., 2004).

The proximal edentulous margin of the dentary and most of the articular border for the predentary are eroded. However, the fact that both of these margins account for less than 25% of the length of the dental battery indicates that the edentulous region of the element was reduced (fig. 7B), as is typical of non-hadrosaurid hadrosaurids such as *Shungmiaosaurus gilmorei* (You et al., 2003b), *Penelopognathus weishampeli* (Godefroit et al., 2005), or *Bactrosaurus johnsoni* (e.g., AMNH FARB 6553). Anteriorly, the ventral margin of the dentary gently deflects

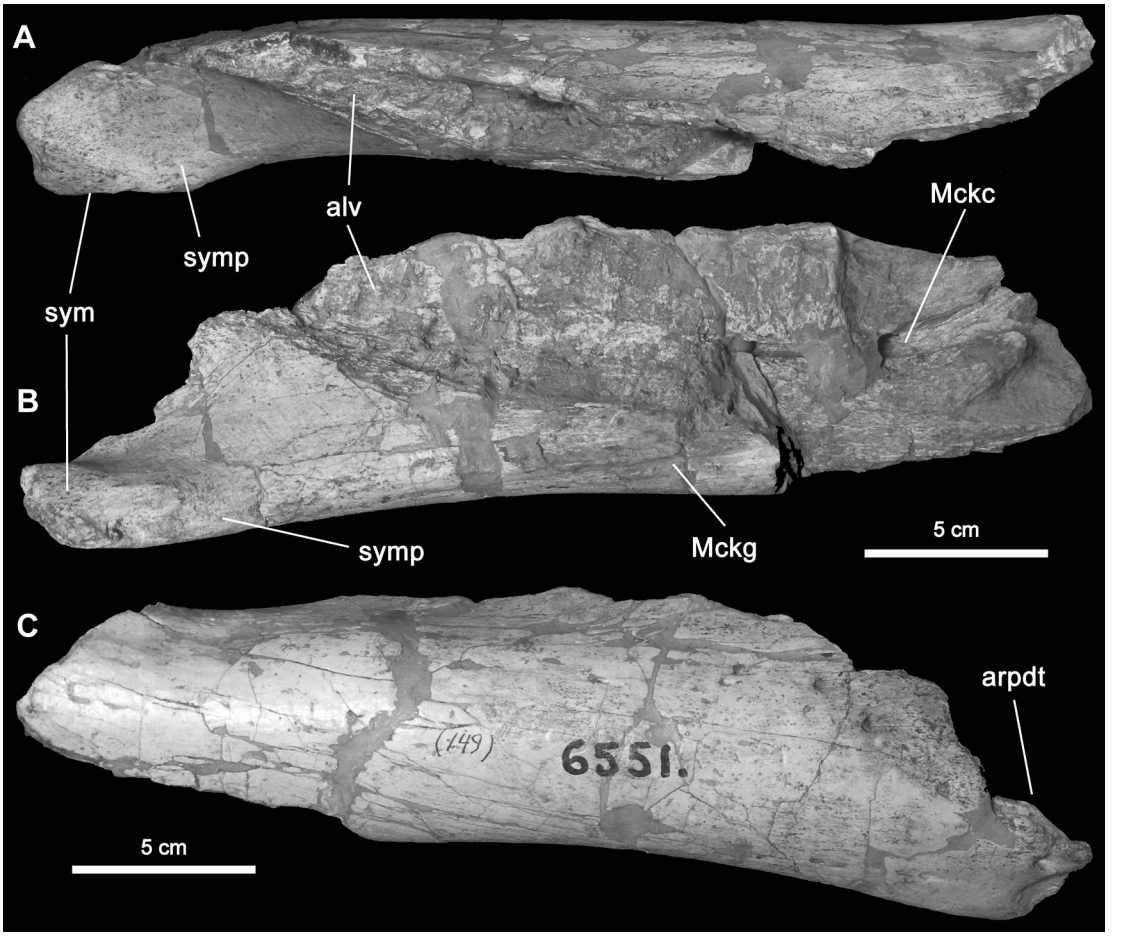

FIGURE 7. Right dentary of *Gilmoreosaurus mongoliensis* (AMNH FARB 30654). **A,** dorsal; **B,** medial; **C,** lateral. Abbreviations in appendix 2.

ventrally, forming an angle of 10° to the horizontal dorsal margin of the medial wall of the dental battery. The Meckelian groove wedges anteriorly on the medial side of the ventral margin of the dentary. The medial projection of the symphyseal process is very reduced. The ratio between its labiolingual extension and the labiolingual width of the dentary is 1.20. As is typical of most non-hadrosaurid hadrosauroids (Prieto-Márquez, 2010), the mandibular symphysis of *G. mongoliensis* is oblique relative to the long axis of the dentary. This is in contrast to the symphysis of the Hadrosauridae, which is set practically parallel to the long axis of the dentary (Prieto-Márquez et al., 2006b). Likewise, the tooth row of *G. mongoliensis* is oriented anterolaterally (fig. 7A), as in non-hadrosaurid hadrosauroids such as *Bactrosaurus johnsoni* (e.g., AMNH FARB 6553), *Eolambia caroljonesa* (Kirkland, 1998: fig. 6), *Penelopognathus weishampeli* (Godefroit et al., 2005), and *Shungmiaosaurus gilmorei* (You et al., 2003b), but unlike the condition seen in Hadrosauridae, where the tooth row is oriented parallel to the lateral wall of the dentary (Prieto-Márquez et al., 2006b).

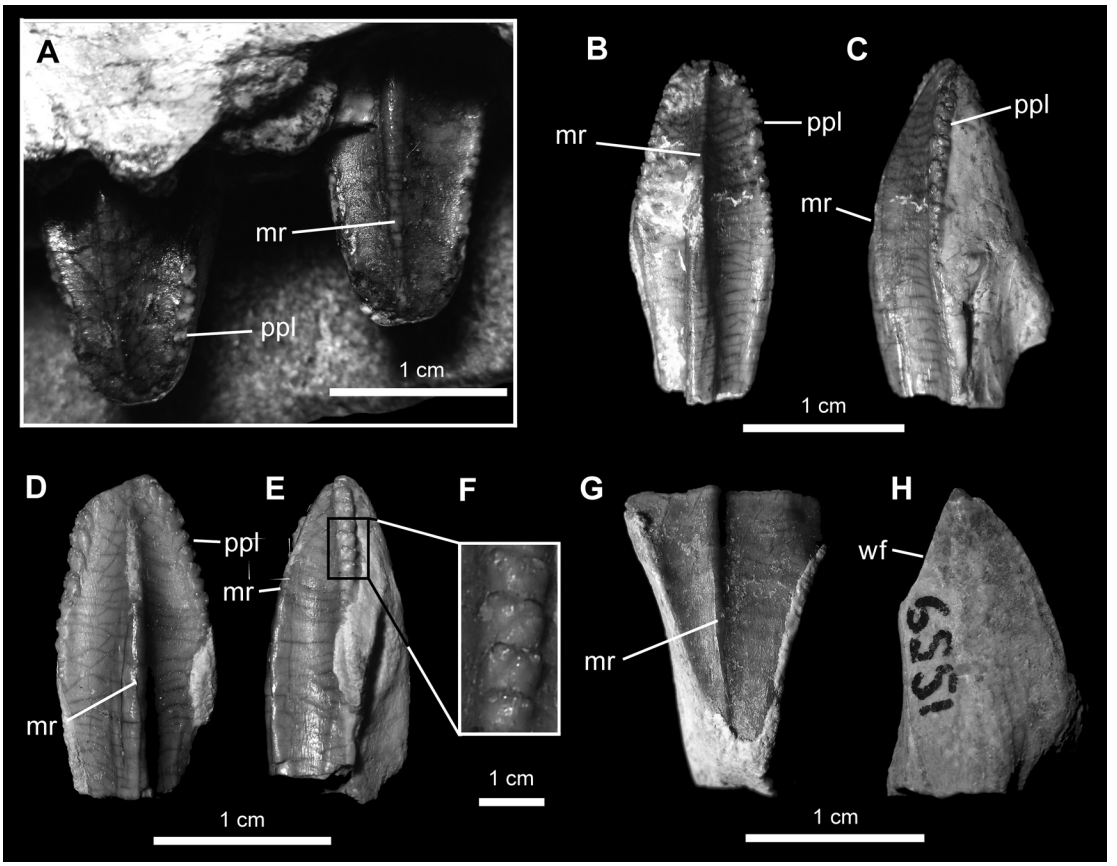

FIGURE 8. Dentition of *Gilmoreosaurus mongoliensis*. **A,** labial view of two tooth crowns from the middle of the dental battery of the right maxilla (AMNH FARB 30653) in figure 1. **B–C,** maxillary tooth crown (AMNH FARB 30662) in labial and marginal views. **D–E,** maxillary tooth crown (AMNH FARB 30663) in labial and marginal views, with **F,** a detail of marginal papillae. **G–H,** dentary tooth crown (AMNH FARB 30661) in lingual and marginal views.

The lateral surface of the dentary is dorsoventrally convex and smooth in texture, bearing a minimum of seven foramina scattered over the anterodorsal and anteroventral surfaces (fig. 7C). The coronoid process and the posterior region of the dentary are not preserved. The posterior extent of the Meckelian canal is exposed medially at the posterior end of the specimen. The exposed segment of this canal is subcylindrical and extends anteriorly at middepth of the dentary.

Dentition: The available dentition of *Gilmoreosaurus mongoliensis* is composed of those teeth still in place in the maxilla (AMNH FARB 30653) and nine isolated tooth crowns (AMNH FARB 30661–30669) (fig. 8). Of the latter, only one is recognizable as a dentary tooth (AMNH FARB 30661; fig. 8G–H). Maxillary tooth crowns have a length/width ratio of 2.75, a measure obtained from the most complete of the isolated crowns (AMNH FARB 30662; fig. 8B–C). There is a single median ridge on the enamel covered labial surface of the maxillary teeth, and no sign of secondary ridges. The median ridge is straight and centered in the middle of the

crown in all the teeth (fig. 8D). A centered ridge is also present in most maxillary teeth of *Shungmiaosaurus gilmorei* (You et al., 2003b), *Lophorhothon atopus* (AUMP 2295), some specimens of *Bactrosaurus johnsoni* (e.g., AMNH FARB 6553), and the Hadrosauridae (Prieto-Márquez, 2010). Denticles are present on the mesial and distal margins and are equal in size, becoming progressively larger toward the apex of the crown. Each denticle forms a ledge composed of a minimum of three knoblike projections. Other hadrosauroids showing similar denticles are *Protohadros byrdi* (SMU 74582) and *Lophorhothon atopus* (AUMP 2295), as well as a number of lambeosaurine hadrosaurids (Prieto-Márquez, 2010). The maxillary occlusal plane of *G. mongoliensis* probably had two functional teeth exposed at midlength along the dental battery. Although no occlusal plane is preserved in the maxilla, in some areas there is one tooth and one empty alveolus arranged mediolaterally, which, combined with the substantial mediolateral breadth of the dental battery, suggests that at midlength of the dental battery there was more than one tooth exposed on the occlusal plane.

The dentary tooth is represented by a worn half crown (AMNH FARB 30661; fig. 8G–H). This tooth crown shows a single ridge that lies off center, closer to one of the margins. Only three minute denticles are present on a very short segment of one of the margins. As in the maxillary teeth, these denticles form ledges composed of at least three knoblike structures. The wear surface of the tooth crown is flat and subtriangular in occlusal view, forming an angle of 60° with the lingual enameled side.

Vertebral Column

The vertebrae of *Gilmoreosaurus mongoliensis* (figs. 9–10) are indistinct from those of other hadrosauroids, which have already been described in detail (Lull and Wright, 1942; Parks, 1920; Godefroit et al., 1998; Prieto-Márquez, 2007). Thus, only a concise description will be provided here, emphasizing those few characters that are phylogenetically informative.

The cervical vertebrae of *Gilmoreosaurus mongoliensis* (AMNH FARB 30671–30673) have centra that are strongly opithocoelous, heart shaped in posterior view, and mediolaterally compressed (fig. 9A–B). The neural canal is large and nearly circular. The postzygapophyseal processes are less than three times as long as the neural arch and are consequently less posteriorly elongate than in the Hadrosauridae, and more like the condition in non-hadrosaurid hadrosauroids (Horner et al., 2004). The centra of the anterior dorsals (AMNH FARB 30674–30680) (fig. 9C–D) are less opisthocoelous and more mediolaterally compressed than the condition in the cervicals. These centra have heart-shaped anterior and posterior facets. The transverse processes are large and long, being oriented laterodorsally and posteriorly. The neural canal is still large in the anteriormost dorsals, but decreases in diameter posteriorly along the series. The neural spines are subrectangular laminae that are posteriorly tilted and become mediolaterally thicker at their distal ends. In the middle and posterior dorsals (AMNH FARB 30681–30685), the neural spines are more vertically oriented and mediolaterally thicker distally. In the most complete posterior dorsal vertebra (fig. 9E–F) the neural spine is slightly more than twice as tall as the centrum. In the middle and posterior dorsal vertebrae the centra remain heart shaped anteriorly and posteriorly, but become anteroposteriorly compressed, with flat anterior

facets and slightly opisthocoelous posterior surfaces. The transverse processes are laterally and slightly dorsally oriented.

The first of the three preserved sacral fragments consists of three coossified vertebrae from the anterior part of the sacrum (AMNH FARB 30688; fig. 10A–C). The centra are platycoelous, relatively elongate, and preserve the heart-shaped anterior profile seen in the dorsal series. A median longitudinal ridge is present on the ventral surface of the centra, as in *Iguanodon bernissartensis* (e.g., IRSNB 1723), *Bactrosaurus johnsoni* (Godefroit et al., 1998), *Claosaurus agilis* (Carpenter et al., 1995), and many other hadrosauroids (Prieto-Márquez, 2008: table G2). The neural canal is relatively large and dorsoventrally elongate. The transverse processes are only partially preserved in the two posterior vertebrae. These processes anteroposteriorly expand at their lateral ends and their ventral surfaces merge with the neural arches via dorsoventrally extensive laminae. Ventrally, at the level of the lateral side of the centra, there is a fragment of the longitudinal bar that unites the sacrum with the medial surface of the ilium. The anterior two centra of this fragment are excluded from the bar. A second sacral fragment preserves four fused neural spines (AMNH FARB 30686; fig. 10D). These spines are anteroposteriorly wider than those of the dorsal vertebrae, and becoming mediolaterally thick distally. The bony laminae that unite the transverse processes to the neural arches are, like the latter, incompletely preserved. A vertical ridge is exposed laterally marking the union of two consecutive neural arches. The third sacral fragment (AMNH FARB 30687) consists of four coossified centra, which are posteriorly twice as wide mediolaterally as the anteriormost centrum of the specimen (fig. 10E). The posterior facet of this series is slightly concave, whereas the anterior one is flat. A ventral sulcus is present on the posterior three centra (fig. 10E). Ventral sulci, like ventral ridges, are intraspecifically variable in Hadrosauroidea (Godefroit et al., 1998; Prieto-Márquez, 2008: table G2).

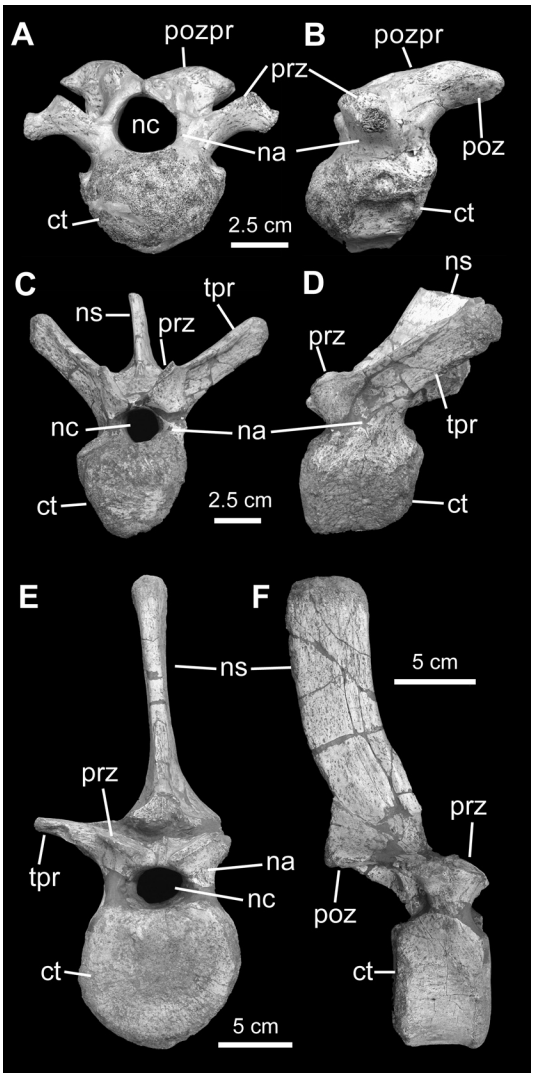

FIGURE 9. Selected axial elements of *Gilmoreosaurus mongoliensis*. **A–B,** cervical vertebra (AMNH FARB 30671) in anterior and left lateral views. **C–D,** anterior dorsal vertebra (AMNH FARB 30678) in anterior and left lateral views. **E–F,** posterior dorsal vertebra (AMNH FARB 30683) in anterior and right lateral views. Abbreviations in appendix 2.

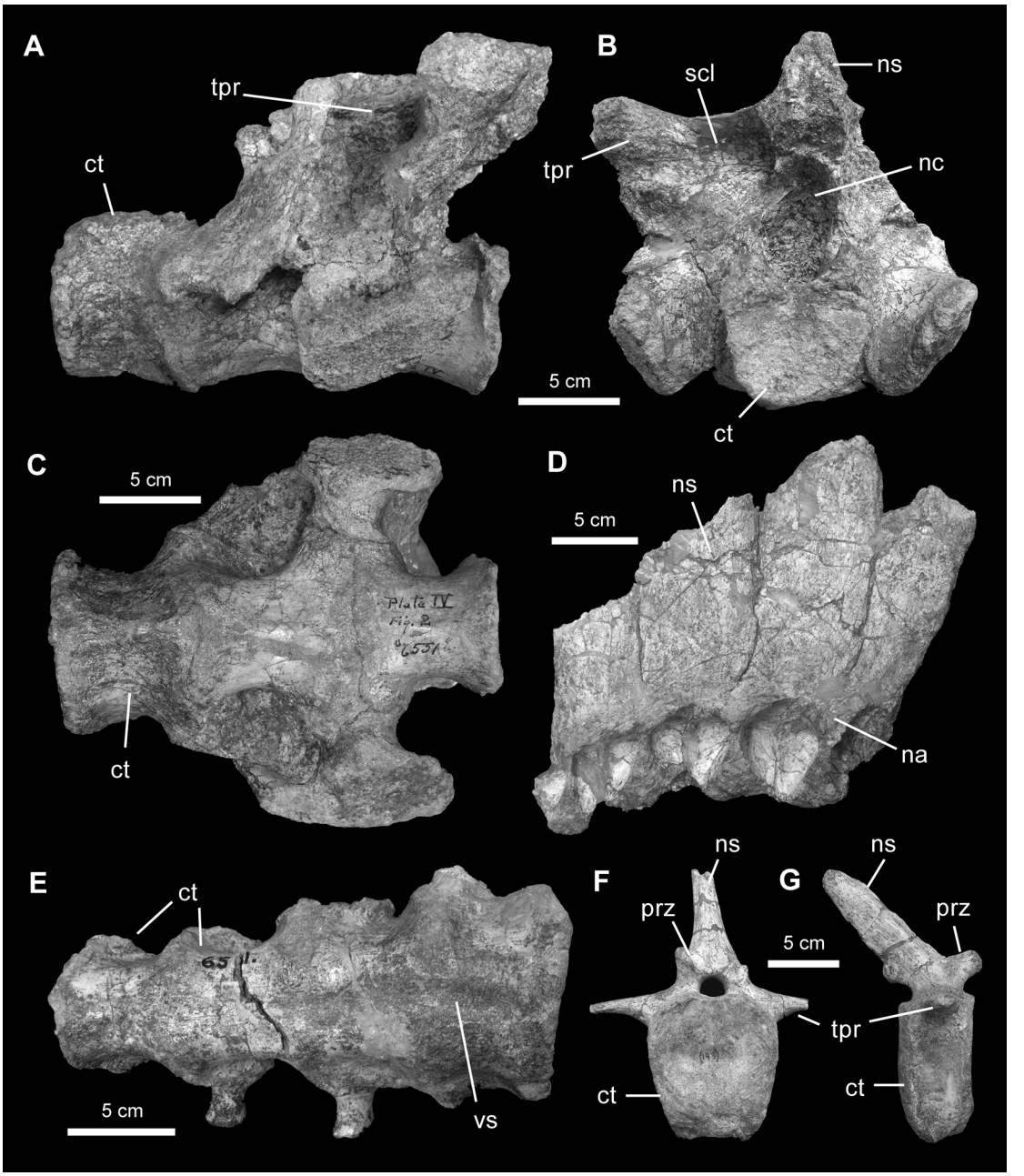

FIGURE 10. Selected axial elements of *Gilmoreosaurus mongoliensis*. **A–C,** partial sacrum (AMNH FARB 30688) in left lateral, posterior, and ventral views, respectively. **D,** neural arches and neuroapophyses of partial sacrum (AMNH FARB 30686) in left lateral view. **E,** coossified sacral centra (AMNH FARB 30687) in ventral view. **F–G,** caudal vertebra from proximal series (AMNH FARB 30689) in anterior and right lateral views. Abbreviations in appendix 2.

As usual in iguanodontians, proximal caudal vertebrae (AMNH FARB 30689–30695) show large anteroporsteriorly compressed centra with hexagonal articular surfaces, proportionally small neural canals, laterally projected transverse processes, and posteriorly oriented neural spines (fig. 10F–G). Distally, caudal vertebrae (AMNH FARB 30696–30721) acquire progressively more elongate centra and neural spines that are gradually more posteriorly oriented.

Pectoral Girdle

Coracoid: The coracoid is a mediolaterally compressed and oval bone (AMNH FARB 30722–30724; fig. 11A–C). Posteriorly, the element is greatly expanded mediolaterally to form the articular facets for the scapula and the humerus (the glenoid fossa). The scapular facet is equilateral and triangular. The glenoid is D-shaped and lies ventral and adjacent to the scapular facet. These facets are approximately equal in length and their lateral margins form an angle greater than 115°, as in *Bactrosaurus johnsoni* (e.g., SBDE/95E), *Lophorhothon atopus* (e.g., AUMP 2295), and *Probactrosaurus gobiensis* (Norman, 2002). A large and slightly elliptical coracoid foramen pierces the coracoid mediolaterally near the junction of the glenoid and scapular facets. The anterodorsal margin of the coracoid is slightly concave (fig. 11B), as in *B. johnsoni* (Godefroit et al., 1998: pl. 10), but much less so than the typical hadrosaurid condition (e.g., *Hypacrosaurus stebingeri,* MOR 553-8-28-5-12). The anterodorsal region of the coracoid is mediolaterally thin and curved medially. The anterior margin of the coracoid, including that of the ventral process, is sinuous. As in basal iguanodontians and non-hadrosaurid hadrosauroids (Horner et al., 2004), the ventral process is relatively short and triangular in lateral view, as well as directed ventrally rather than hooked posteroventrally (fig. 11A–C).

Scapula: The scapula of *Gilmoreosaurus mongoliensis* has a relatively straight dorsal profile (AMNH FARB 30725–30727; fig. 11E–G), as in non-hadrosaurid hadrosauroids except *Tanius sinensis* (Prieto-Márquez, 2010). The long axis of the scapula is gently curved anteromedially. The medial surface of the element is flat throughout most of its length, becoming dorsoventrally convex proximally. The distal blade is only moderately expanded, so that its maximum breadth is less than the width of the proximal region (between the ventral process of the glenoid and the pseudoacromion process). This condition is typical in non-hadrosaurid hadrosauroids except *Bactrosaurus johnsoni* (e.g., AMNH FARB 6553), where, as in hadrosaurids (Prieto-Márquez, 2008: fig. H10), the distal end of the scapular blade is broader than the proximal region. The proximal constriction, the area of the scapula lying between the proximal region and the distal blade, is very narrow; its breadth is about half the width of the proximal region. The pseudoacromion process is slightly oriented dorsally at its anterior end, as is commonly observed in non-hadrosaurid hadrosauroids and in lambeosaurine hadrosaurids (Prieto-Márquez, 2010). The deltoid ridge is well developed and extends obliquely from the posteroventral margin of the pseudoacromion process to the ventral margin of the scapular blade. The coracoid facet is concave and subrectangular. Its lateral margin forms an angle of 125° with the dorsal segment of the lateral margin of the glenoid. The latter facet is also concave and twice as long as it is mediolaterally wide. Likewise, the glenoid facet is also dorsoventrally curved and its ventral end is triangular and mediolaterally expanded.

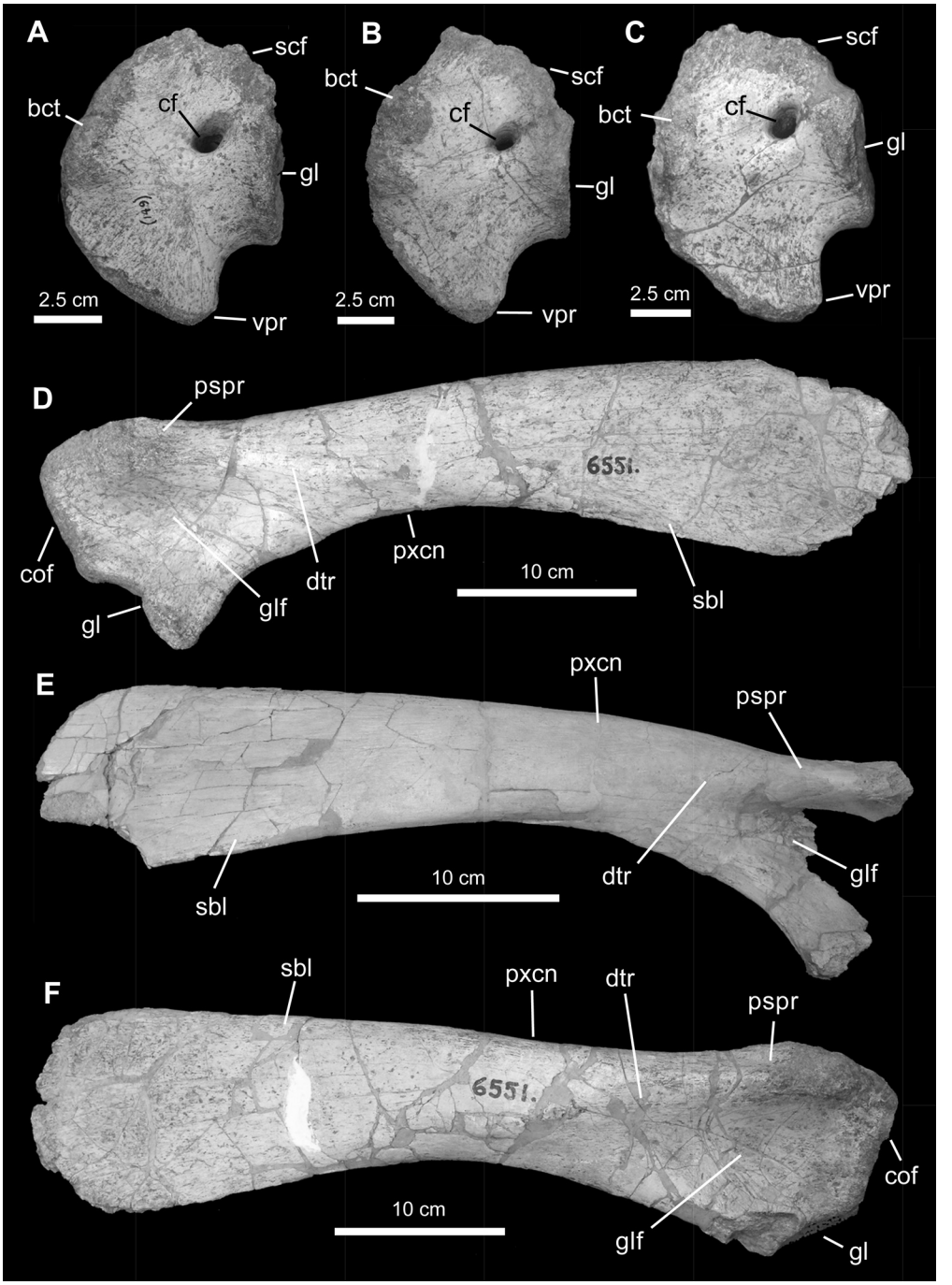

FIGURE 11. Pectoral girdle elements of *Gilmoreosaurus mongoliensis.* **A–C,** left lateral views of three coracoids (AMNH FARB 30722, 30723, and 30724). **D–F,** lateral views of left (AMNH FARB 30725), partial right (AMNH FARB 30726), and nearly complete right (AMNH FARB 30727) scapulae. Abbreviations in appendix 2.

Forelimb

Humerus: The humerus is proportionately short and robust (AMNH FARB 30728; fig. 12A–B). The articular head is mediolaterally expanded and proximally offset relative to its proximolateral corner. The deltopectoral crest projects lateroventrally from the proximal half of the humerus. With a maximum width/anteroposterior diameter of the humeral shaft ratio of 1.67, the lateroventral extension of the deltopectoral crest is comparable to that of the non-hadrosaurid hadrosauroids *Bactrosaurus johnsoni* (e.g., SBDE 95E/24) and *Tanius sinensis* (e.g., PMU R235), and several hadrosaurids, such as *Edmontosaurus annectens* (e.g., AMNH FARB 5879) and *Gryposaurus latidens* (AMNH FARB 5465). However, the crest is relatively short proximodistally, with a crest length/humeral length ratio of 0.43. Deltopectoral crests that are shorter than half the length of the humerus are also present in basal iguanodontians, the non-hadrosaurid hadrosaurids *Bactrosaurus johnsoni, Tanius sinensis, Lophorhothon atopus,* and the hadrosaurid *Hadrosaurus foulkii* (Prieto-Márquez, 2008: fig. H15). The lateral margin of the deltopectoral crest greatly thickens toward its ventral margin, which is relatively rounded as in non-hadrosaurid iguanodontians except *Nanyangosaurus zhugeii* (Xu et al., 2000).

The humeral shaft is elliptical in cross section and slightly compressed mediolaterally. A prominent median tuberosity is present on the posterior surface of the humerus one-third the distance from the proximal terminus (fig. 12A). The distal end of the humerus is mediolaterally expanded to form lateral ulnar and medial radial condyles. The ulnar condyle is wider and more anteroposteriorly expanded than the radial condyle. A shallow depression separates the two condyles on the anterior and posterior surfaces of the distal end of the humerus.

Radius: The radius is subcylindrical (AMNH FARB 30729; fig. 12C–D), with expanded proximal and distal ends. This bone articulates with and matches the size of the left ulna (AMNH FARB 30729; fig. 12E–F), so that they probably correspond to the forearm of the same individual. The proximal region of the radius is expanded in all directions, but slightly more so mediolaterally. The ventral surface is flat and triangular, with longitudinal striations. This triangular surface rests on the dorsal surface of the proximal ulnar surface. A long ridge extends distally from the apex of this proximoventral articular surface and extends to the distal end of the radius. The proximal surface of the radius is slightly concave and triangular. The shaft of the radius increases in depth more gently toward the distal end than it does proximally. The distal end is also triangular in cross section, but deeper dorsoventrally than it is mediolaterally wide. A flat surface that faces lateroventrally represents the articulation with the mediodorsally facing articular distal end of the ulna. The articular distal surface of the radius is triangular and marked with striations. It is twice as long as the proximal articular surface.

Ulna: With a length/dorsoventral width ratio slightly greater than 10, the ulna of *Gilmoreosaurus mongoliensis* (AMNH FARB 30729; fig. 12E–F) is a relatively short element compared with other hadrosauroid taxa (Prieto-Márquez, 2008: fig. H19). The ulna is expanded at its proximal and distal ends. Proximally, it is at least twice as expanded mediolaterally as it is dorsoventrally. The dorsal surface of the proximal third of the ulna shows a gentle depression for reception of the proximal radius. The lateral flange is thick and projects dorsolaterally above the main shaft of the ulna. The medial flange is dorsoventrally compressed but further expanded

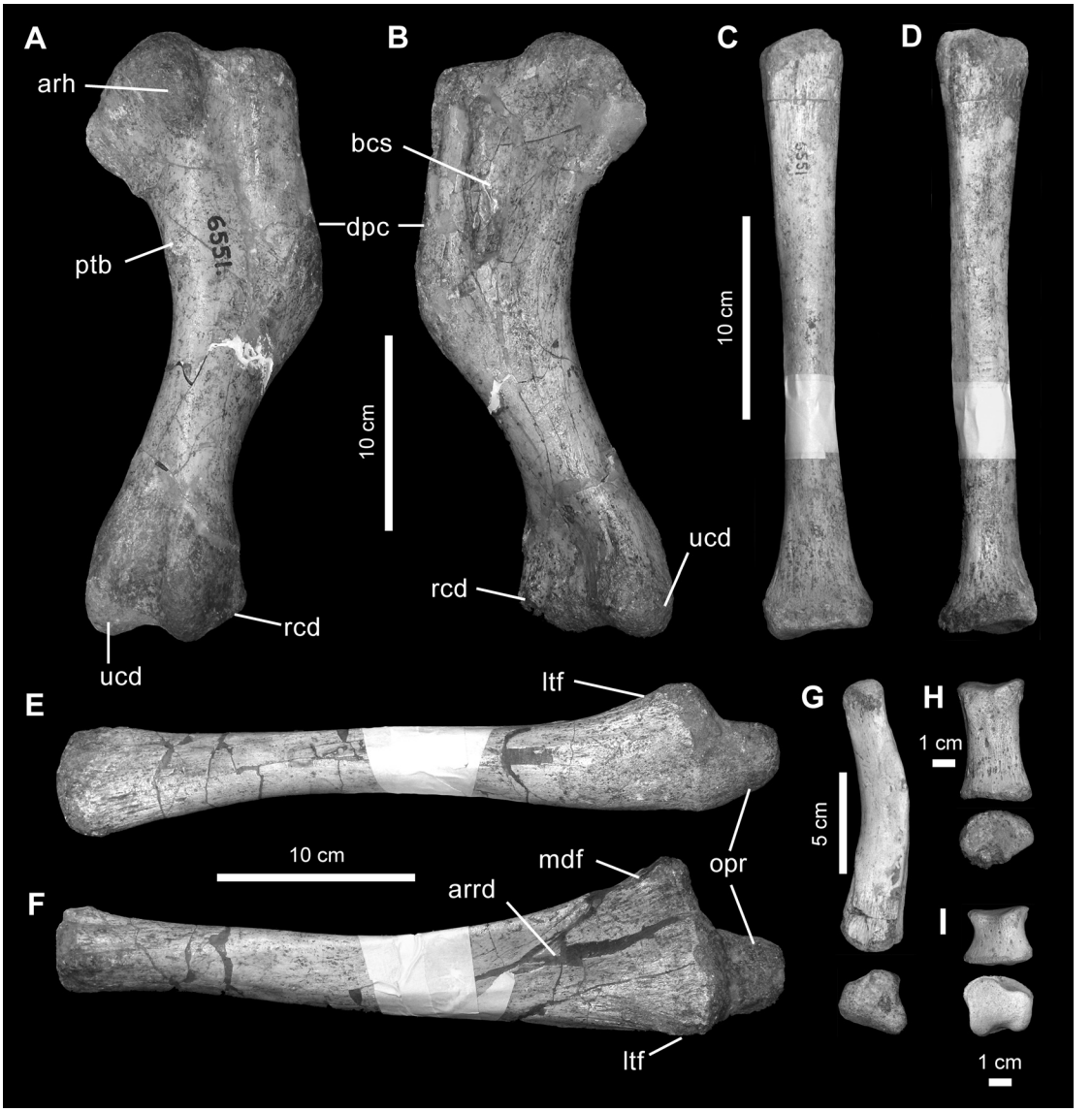

FIGURE 12. Forelimb elements of *Gilmoreosaurus mongoliensis.* **A–B,** right humerus (AMNH FARB 30728) in posterolateral and anteromedial views. **C–D,** left radius (AMNH FARB 30729) in lateral and dorsal views. **E–F,** left ulna (AMNH FARB 30729) in lateral and dorsal views. **G,** left metacarpal IV (AMNH FARB 30730) in dorsal view, with its proximal articular surface shown below. **H,** right manual phalanx II-1 (AMNH FARB 30732) in dorsal view, with its proximal articular surface shown below. **I,** right manual phalanx III-1 (AMNH FARB 30733) in dorsal view, with its distal articular surface shown below. Abbreviations in appendix 2.

dorsolaterally than the lateral flange. Its medial surface is strongly concave. A shallow and short ridge is present on the dorsal margin of the distal region of the medial flange. The olecranon process is thick and dorsoventrally compressed, with a flat dorsal surface, a mediolaterally convex ventral side, and an elliptical proximal articular facet.

The middle and distal regions of the shaft change from being mediolaterally wider to become more expanded dorsoventrally near the distal end of the ulna. The latter is nearly as deep as the proximal end of the element. The distal fifth of the ulna has a flat articular surface for the radius that faces mediodorsally and shows longitudinal striations. In addition to this flat surface, two other dorsoventrally convex surfaces (one lateral and the other medioventral) complete the distal region of the ulna, which displays a subtriangular cross section.

Metacarpal IV: This manual element (AMNH FARB 30730 and 30731) is composed of a short shaft that is dorsoventrally compressed throughout its proximal two-thirds and mediolaterally compressed along the distal third (fig. 12G). The proximal articular surface is triangular and slightly convex. The medial and ventral surfaces of the proximal third of metacarpal IV show a large triangular and shallow depression. The proximoventral margin of the medial surface extends further medially than the proximodorsal margin. The metacarpal is dorsoventrally compressed at midshaft, showing a flat ventral surface and a mediolaterally convex and laterally sloping dorsal surface. The medial surface of the distal third of the metacarpal is slightly concave and terminates in a vertical mediodistal margin. The distal end is mediolaterally compressed, so that its distal articular surface is twice as high as it is wide. In distal view, the straight vertical medial margin and the convex lateral margin converge dorsally to a point, whereas ventrally they are separated by a mediolaterally narrow ventral border.

In *Gilmoreosaurus mongoliensis* metacarpal IV is proportionately short, with a ratio between the total length and the width of the dorsal surface at midshaft of 5.5. This value is comparable to that of basal iguanodontians (e.g., *Iguanodon bernissartensis,* IRSNB 1534 has a ratio of 4.35), but is substantially lower than in the Hadrosauridae (e.g., *Tsintaosaurus spinorhinus,* IVPP V725, ratio of 9; *Maiasaura peeblesorum,* ROM 44770, ratio of 8.7). Examples of metacarpal IV are rare among non-hadrosaurid hadrosauroids. *Lophorhothon atopus* (e.g., AUMP 2295) and *Probactrosaurus gobiensis* (Norman, 2002: fig. 24) have relatively longer metacarpal IVs, with length/width ratios of 7. Examination of casts of metacarpals II and III referred to *Bactrosaurus johnsoni* by Godefroit et al. (1998) (SBDE 95E sample) showed relatively short elements, with similar proportions than the metacarpal IV of *G. mongoliensis.* Since at least metacarpals III and IV exhibit similar proportions in the iguanodontian manus (Horner et al., 2004; Norman, 2004), it is likely that the length/width ratio of these elements in *G. mongoliensis* and *B. johnsoni* are similar, representing the shortest known metacarpals within Hadrosauroidea.

Manual Phalanges: The manus is represented by two proximal phalanges, II-1 and III-1. As in the case of metacarpal IV, both phalanges are proportionately shorter than in at least some non-hadrosaurid hadrosauroids, such as *Probactrosaurus gobiensis* (Norman, 2002: fig. 25–26), and the Hadrosauridae (e.g., *Hypacrosaurus altispinus,* AMNH FARB 5357, or *Brachylophosaurus canadensis,* MOR 794). Phalanx II-1 (AMNH FARB 30732; fig. 12H) is dumbbell shaped and dorsoventrally compressed. It is twice as long as it is wide across its broader dorsal surface. The proximal surface is slightly concave, with a crescentic laterodor-

sal margin, a straight medial border, and a convex ventral margin. A rugose ridge extends from the proximal margin on the ventromedial surface of the bone. The distal surface is suboval and slightly concave throughout most of its area, except for a convex lateroventral corner.

Phalanx III-1 (AMNH FARB 30733; fig. 12I) is a quadrangular and proximodistally short bone. Its dorsal, medial, lateral, and palmar surfaces are proximodistally convex. The proximal articular surface is slightly convex and very asymmetric due to the much deeper lateral margin. This asymmetry is greater on the saddle-shaped distal surface, where its lateral portion is approximately 40% deeper and than the medial one (fig. 12I). The proximal and, especially, the distal asymmetrical configuration of phalanx III-1 are far greater than the slight asymmetric profiles seen in hadrosaurids (e.g., *Maiasaura peeblesorum,* ROM 44770, or *Hypacrosaurus altispinus,* 5357). Phalanx III-1 is also remarkable in possessing a relatively deep extensor groove on the ventral and, to a lesser extent, the dorsal margins of the distal surface. This condition has also been reported in *Bactrosaurus johnsoni* (Godefroit et al., 1998).

Pelvic Girdle

Ilium: The ilium of *Gilmoreosaurus mongoliensis* (AMNH FARB 30734–30737) is proportionately long and shallow (fig. 13). The preacetabular process is long and strongly deflected anteroventrally, forming an angle of 146° with a horizontal line uniting the base of the pubic and ischial peduncles. The proximal region of the preacetabular process is relatively deep, as in most hadrosauroids except *Equijubus normani, Probactrosaurus gobiensis,* and *Claosaurus agilis* (Prieto-Márquez, 2008: fig. I4), accounting for 60% of the total depth of the anterior region of the iliac central plate at the level of the pubic peduncle. The iliac plate is relatively shallow, being 70% as deep as it is anteroposteriorly wide. This proportion reflects a relatively shallow iliac plate compared to that of many hadrosauroids, where the height/width ratio is greater than 0.8 (Prieto-Márquez, 2010).

The dorsal margin of the ilium varies from straight to gently concave above the supraacetabular process from one specimen (AMNH FARB 30735; fig. 13B) to another (AMNH FARB 30736; fig. 13D). The supraacetabular process is asymmetrically V-shaped in profile and is skewed posteriorly in lateral view (fig. 13B, D). The process is as long anteroposteriorly as 75%–80% of the width of the central plate of the ilium, as in *Bactrosaurus johnsoni* (e.g., SBDE/95E). Its lateroventral projection is moderate, reaching about 30% of the depth of the ilium. A similar degree of projection is only observed in *Bactrosaurus johnsoni* (e.g., SBDE/95E) and the lambeosaurine *Velafrons coahuilensis* (e.g., CPC uncatalogued specimen, Prieto-Márquez, unpublished data); in other hadrosauroids the supraacetabular process is projected either less than 25% or more than half the depth of the iliac plate (Prieto-Márquez, 2010). The supraacetabular process extends well into the proximal region of the postacetabular process, so that its ventral apex lays posterodorsal to the ischial peduncle, a condition typically present in basal iguanodontians (e.g., *Iguanodon bernissartensis,* IRSNB 1534) and all non-hadrosaurid hadrosauroids (Prieto-Márquez, 2010). In contrast, in the Hadrosauridae the ventral apex of the supraacetabular process is located anterodorsal to the ischiac peduncle (Brett-Surman and Wagner, 2007).

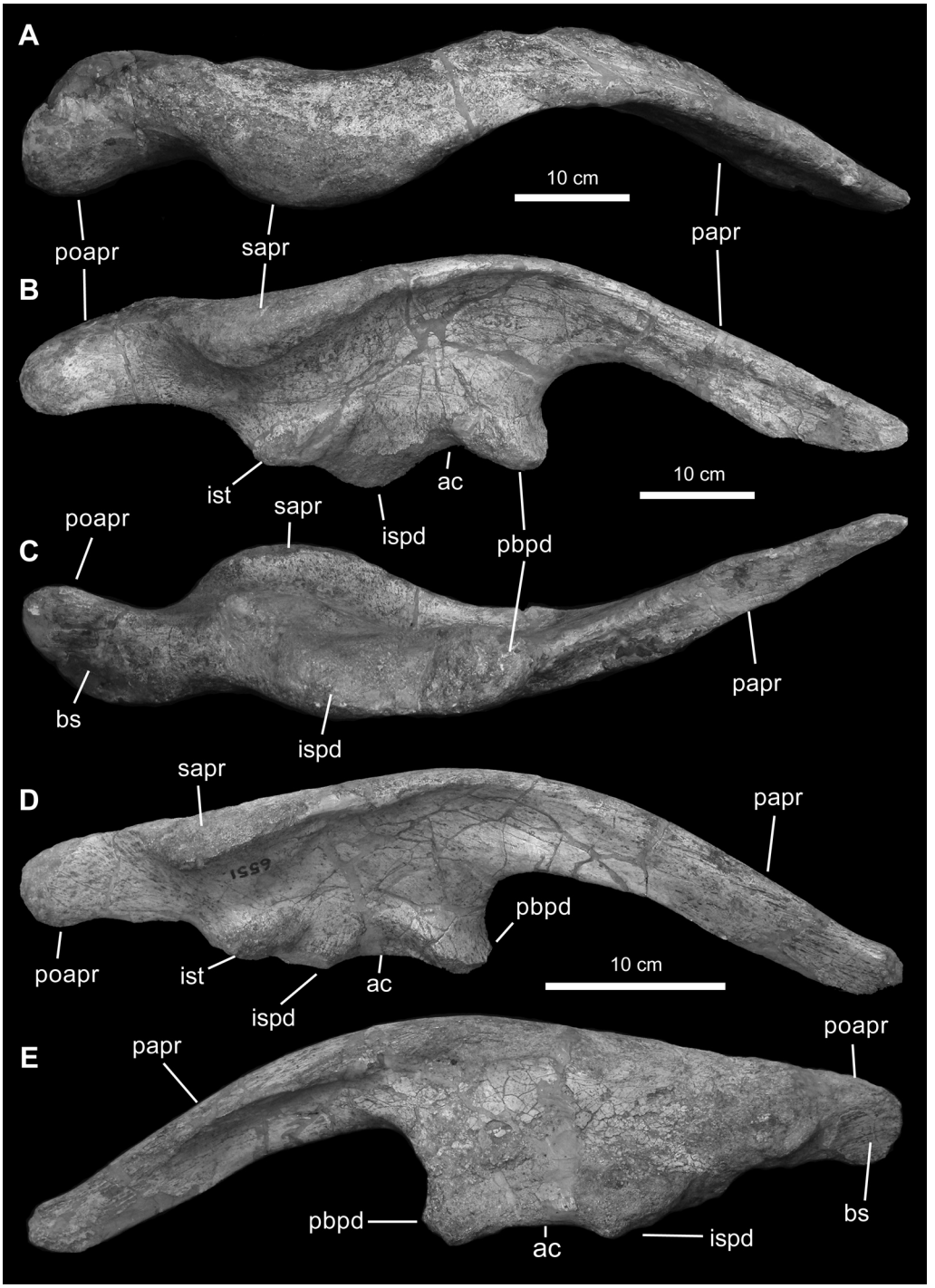

FIGURE 13. Selected pelvic elements of *Gilmoreosaurus mongoliensis.* **A–C,** right ilium (lectotype, AMNH FARB 30735) in dorsal, lateral, and ventral views. **D–E,** right ilium (AMNH FARB 30736) in lateral and medial views. Abbreviations in appendix 2.

The acetabular margin is arcuate and bounded by the pubic peduncle anteriorly and the ischiac peduncle posteriorly. The pubic peduncle is triangular and mediolaterally expands, more so proximally than distally, as in *Bactrosaurus johnsoni, Tanius sinensis, Eolambia caroljonesa, Lophorhothon atopus,* and the Hadrosauridae (Horner et al., 2004). The ischiac peduncle shows a well-developed posterodorsal tuberosity (fig. 13B, D). This feature is absent in non-hadrosaurid iguanodontians, which have a single undivided ischiac peduncle, but is always present in hadrosaurids (Brett-Surman, 1975; Godefroit et al., 2001). Notably, *Tanius sinensis* (PMU R242) and one specimen of *Bactrosaurus johnsoni* (SBDE 95E/25) are the only non-hadrosaurid iguanodontians that show an incipient, small posterodorsal tuberosity, and may represent a transitional state toward the evolution of this feature in hadrosaurids.

The postacetabular process of *Gilmoreosaurus mongoliensis* is unique among iguanodontians in being both relatively short (less than 70% of the length of the iliac central plate) and paddle shaped in lateral profile (fig.13B, D). Other iguanodontians with a short postacetabular process have a triangular lateral profile (e.g., *Mantellisaurus atherfieldensis,* IRSNB 1551) or it is paddle shaped and more than 70% of the length of the iliac plate (e.g., *Brachylophosaurus canadensis,* MOR 794, or *Parasaurolophus cyrtocristatus,* FMNH P27393). *G. mongoliensis* has a brevis shelf on the ventral surface of the postacetabular process (fig. 13C). The shelf faces medioventrally and becomes more expanded posteriorly (fig. 13E). As in all hadrosauroids except *Tanius sinensis* (Prieto-Márquez, 2010), the medial sacral ridge is located within the dorsal third of the central plate. However, as in all non-hadrosaurid hadrosauroids (excluding *Lophorhothon atopus*) the sacral ridge is anteroposteriorly oriented parallel to the dorsal margin of the ilium (fig. 13E).

Ischium: The ischium (AMNH FARB 30739 and 30740) has an anteroposteriorly wide and robust iliac peduncle (fig. 14A–B). Its anterior and posterior margins are slightly convergent dorsally. The posterodorsal corner of the iliac peduncle is slightly recurved posteriorly, forming a thumb-shaped expansion that is nearly as developed as in lambeosaurine hadrosaurids (Wagner, 2001; Brett-Surman and Wagner, 2007). This condition is typical of, although to a lesser degree, non-hadrosaurid iguanodontians, such as *Ouranosaurus nigerensis* (Taquet, 1976) or *Bactrosaurus johnsoni* (e.g., AMNH FARB 6553). The pubic peduncle is very broad anteroposteriorly and strongly compressed mediolaterally. Its articular surface faces anteroventrally as commonly occurs in lambeosaurine hadrosaurids and non-hadrosaurid hadrosauroids (Prieto-Márquez, 2008: fig. I45). The obturator process is strongly compressed mediolaterally and projects ventrally from the proximal region of the ischium. This process is subrectangular, twice as long as it is wide, and medially convex. The ischial shaft is moderately thick, having a midshaft diameter that is 7% of the length of the shaft. The distal end of the shaft is ventrally expanded into the "foot-like" process that is so characteristic of non-saurolophine iguanodontians (Horner et al., 2004; Norman, 2004). Although its ventral margin is eroded, enough is preserved to conclude that, as in non-hadrosaurid iguanodontians, it is less expanded ventrally than in lambeosaurines.

Pubis: The single available pubis (AMNH FARB 30738; fig. 14C–D) does not preserve the anterior margin and anteroventral region of the prepubic process, the shaft of the postpubic process, most of the ischial peduncle, and the dorsal margin of the iliac peduncle. The dorsal

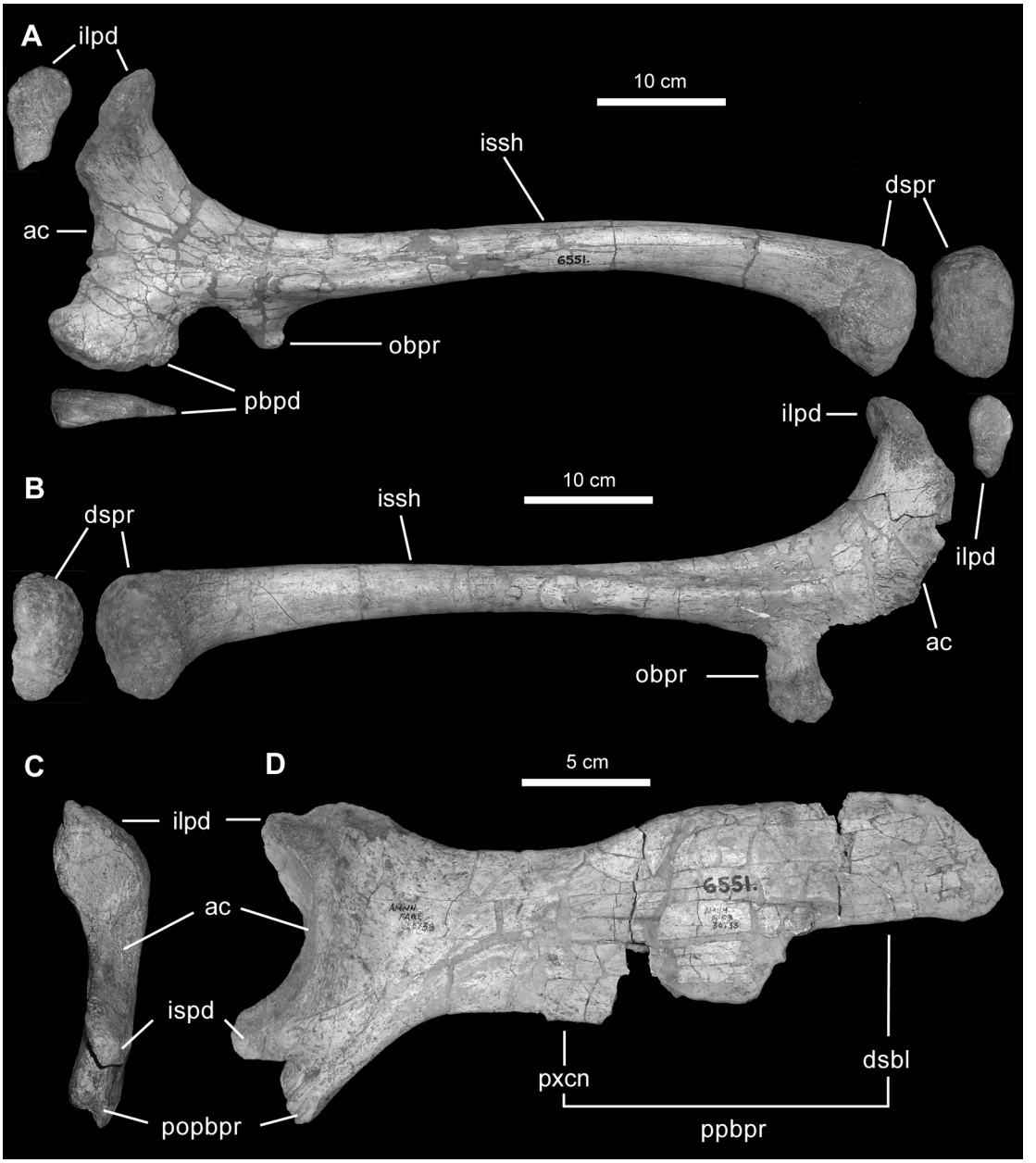

FIGURE 14. Selected pelvic elements of *Gilmoreosaurus mongoliensis*. **A,** left ischium (AMNH FARB 30739) in lateral view, with articular surfaces of the iliac and pubic peduncles, and the distal process. **B,** right ischium (AMNH FARB 30740) in lateral view, with articular surfaces of the iliac peduncles and the distal process. **C–D,** right pubis (AMNH FARB 30738) in posterior and lateral views, respectively. Abbreviations in appendix 2.

margin of the prepubic process lies slightly below the level of the preserved dorsal margin of the iliac peduncle. Unless the missing ventral region of the prepubic blade is much more expanded than the dorsal region, the distal region of the prepubic process does not appear to be dorsoventrally deeper then the width of the acetabular margin of the pubis. The proximal constriction is relatively broad. Its length is similar to that of the distal blade of the prepubic process, as in the non-hadrosaurid hadrosauroid *Lophorhothon atopus* (e.g., AUMP 2295) and several saurolophine (sensu Prieto-Márquez, 2010) hadrosaurids (e.g., *Gryposaurus latidens,* AMNH FARB 5465, or *Secernosaurus koerneri,* MACN RN 2).

The iliac peduncle is tetrahedral and, as preserved, relatively narrow mediolaterally. In the acetabular region, the lateral margin of the iliac peduncle extends ventrally forming a prominent ridge that merges with the proximal region of the ischiac peduncle (fig. 14D). Such a ridge is typically present in non-hadrosaurid iguanodontians (e.g., *Bactrosaurus johnsoni,* AMNH FARB 6553, or *Mantellisaurus atherfieldensis,* IRSNB 1551). The proximal segment of the postpubic process is posteroventrally oriented forming an angle of 140° with the long axis of the prepubic process. The ischiac peduncle is medially offset relative to the postpubic process and its dorsal surface contributes to the arcuate lateral profile of the acetabular margin of the pubis.

Hind Limb

Femur: The femur is slightly curved medially (AMNH FARB 3074; fig. 15A). The medially projecting articular head lies proximally. The anterior trochanter is long and relatively large, being anteriorly offset and separated from the lateral surface of the proximal femur by a deep cleft. The femoral shaft is slightly compressed anteroposteriorly. The fourth trochanter extends along the middle third of the posterior surface of the shaft, near its medial side. It is low and its triangular profile is asymmetrical and distally skewed (fig. 15B). The distal region of the femur is mostly anteroposteriorly expanded to form the medial and lateral condyles, which are separated anteriorly and posteriorly by intercondylar grooves (fig. 15A, C).

Tibia: The tibia is the most abundant element in the sample of bones of *Gilmoreosaurus mongoliensis* (fig. 16) represented by six elements (AMNH FARB 30742–30747). It is a robust element composed of a subcylindrical shaft that is anteroposteriorly expanded proximally and mediolaterally expanded distally. As in other hadrosauroids (Godefroit et al., 2001), the cnemial crest is relatively long proximodistally, extending into the proximal third of the tibia (fig. 16B). At the distal of the tibia, the external malleolus is greatly offset ventrally relative to the internal malleolus. The triangular excavation between the two malleoli, for reception of the anterior ascending process of the astragalus, is deep and well developed.

The much smaller juvenile tibiae of *Gilmoreosaurus mongoliensis* (AMNH FARB 30743–30745) differ little from that of the larger (perhaps adult) individuals in the sample. In juveniles, the ventral offset of the external malleolus is less developed (fig. 16E). The distal margin of the cnemial crest, near the area where it merges with the anterior surface of the tibia, is less pronounced and not as sharply defined as in the larger specimens (fig. 16E). Likewise, the internal condyle at the proximal end of the tibia is less prominent in juveniles (fig. 16G).

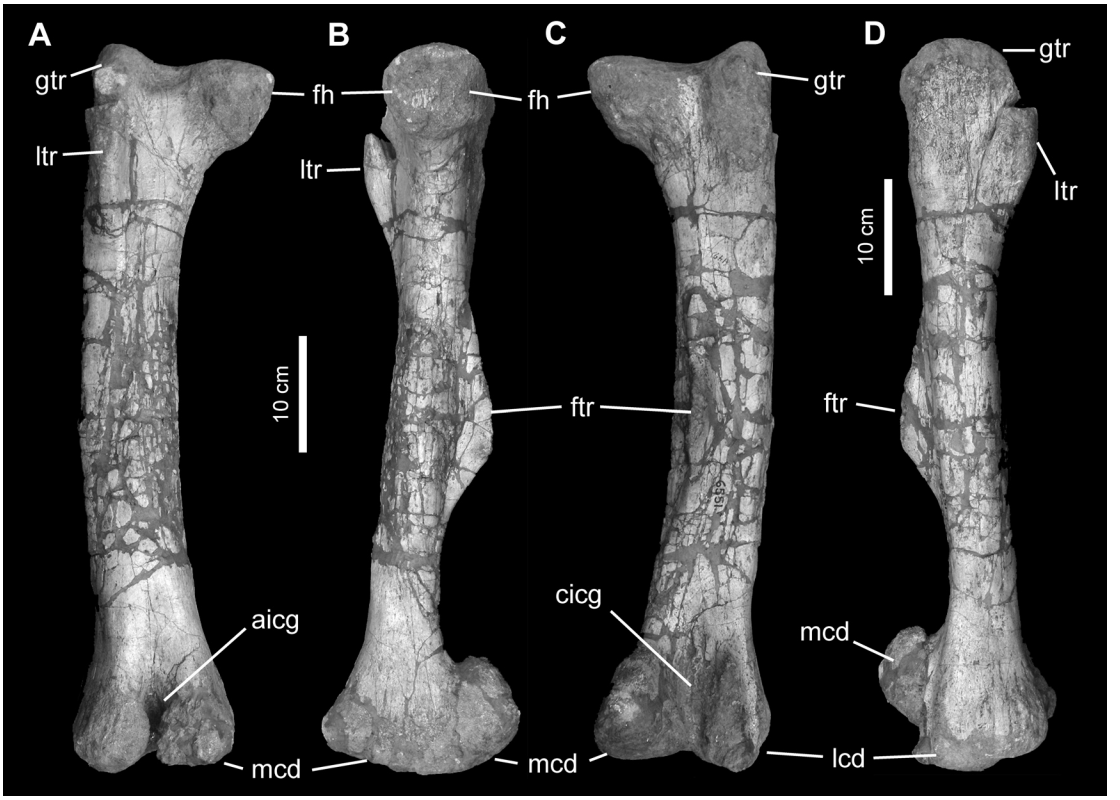

FIGURE 15. Right femur of *Gilmoreosaurus mongoliensis* (AMNH FARB 30741). **A,** anterior; **B,** medial; **C,** posterior; **D,** lateral. Abbreviations in appendix 2.

Fibula: The fibula (AMNH FARB 30748 and 30749) is long and slender (fig. 17A–B). The bone is mediolaterally compressed and anteroposteriorly expanded. The anteroposterior expansion occurs very gradually toward the proximal end but abruptly at the distal end. The lateral surface of the fibula is anteroposteriorly convex, whereas the medial side bears a long depression along the proximal half of the shaft. The medial surface of the distal region of the fibula shows a flat articular surface that is oriented obliquely in relation to the proximal two-thirds of the fibula.

Astragalus: The saddle-shaped astragalus (AMNH FARB 30750–30752) is the largest of the proximal tarsals (fig. 17G–H). The extensive dorsal surface is for the most part covered medially by the concave articular surface for the tibia. The bone is anteroposteriorly widest across the medial margin. The latter becomes progressively thicker posteriorly, toward the posterior ascending process. This process is triangular and projects dorsomedially, contributing to the medially skewed posterior profile of the astragalus. Similarly, the anterior surface of the element contains the triangular anterior ascending process, which is deeper than the posterior ascending process and largely contributes to the laterally skewed anterior profile of the element. The astragalus is anteroposteriorly constricted at the level of the anterior ascending process.

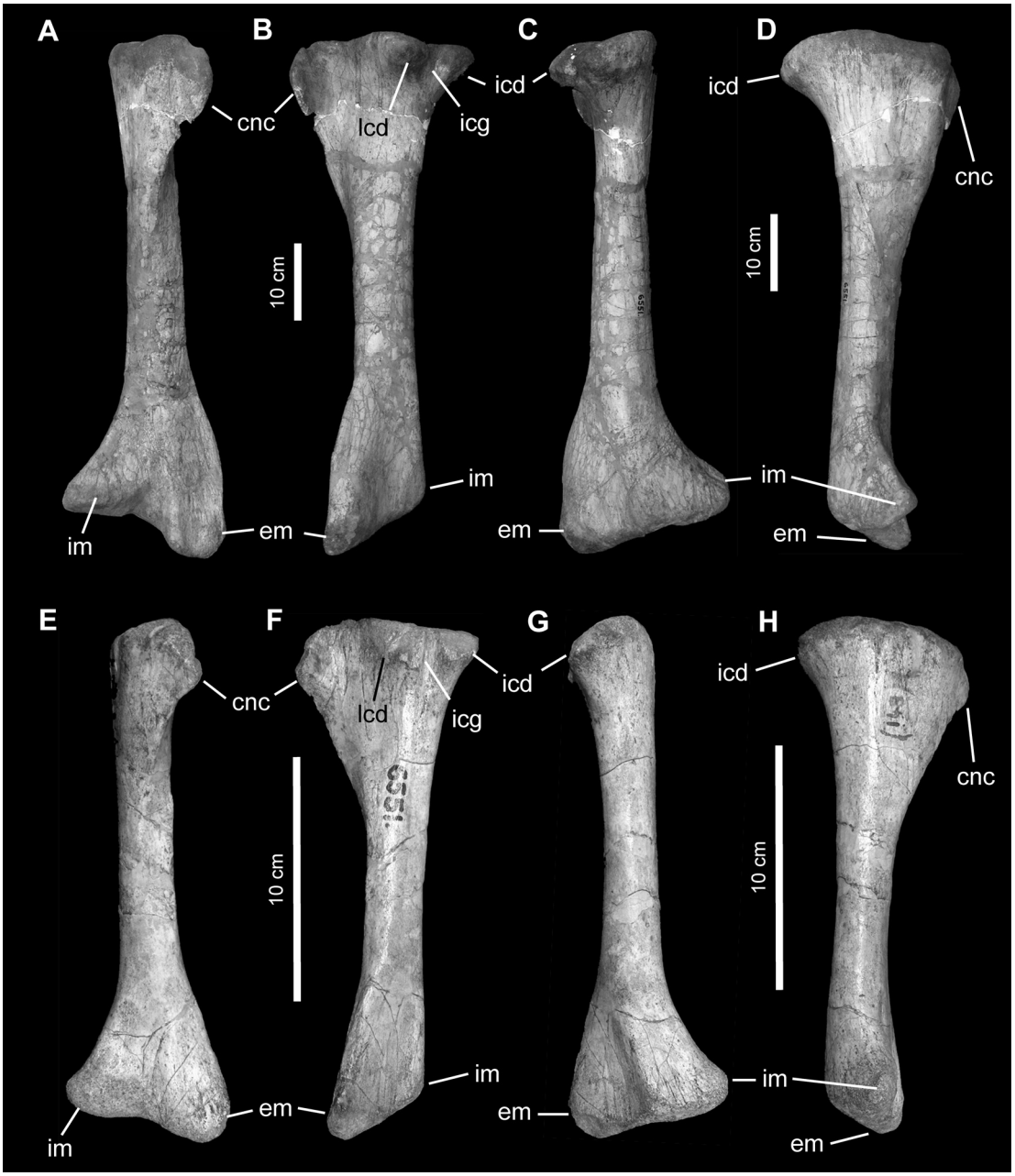

FIGURE 16. Tibiae of *Gilmoreosaurus mongoliensis.* **A–D,** left tibia (AMNH FARB 30742) in anterior, lateral, posterior, and medial views. **E–H,** left juvenile tibia (AMNH FARB 30743) in anterior, lateral, posterior, and medial views. Abbreviations in appendix 2.

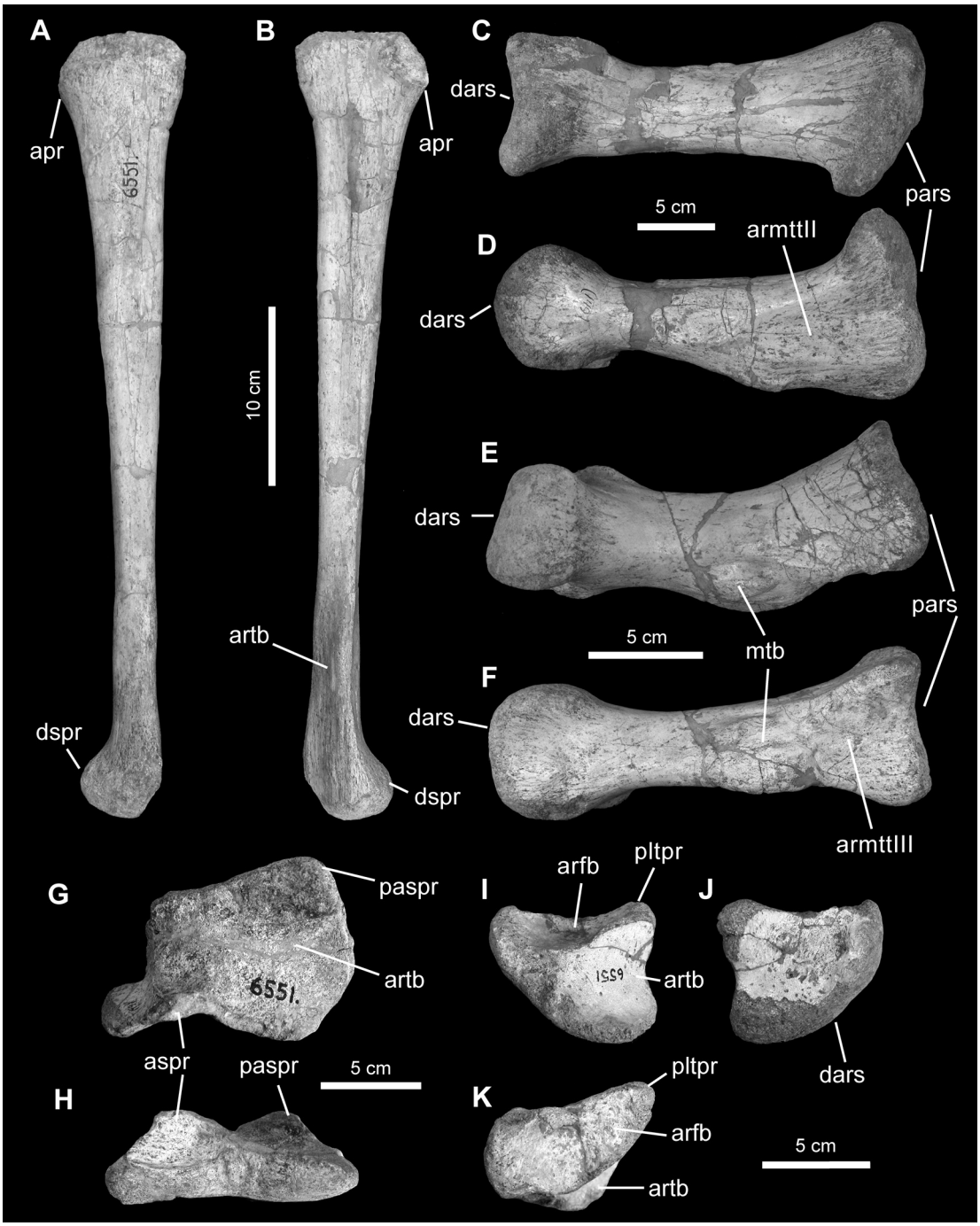

FIGURE 17. Hind-limb elements of *Gilmoreosaurus mongoliensis.* **A–B,** left fibula (AMNH FARB 30748) in lateral and medial views. **C–D,** left metatarsal III (AMNH FARB 30754) in dorsal and medial views. **E–F,** right metatarsal IV (AMNH FARB 30756) in dorsal and medial views. **G–H,** right astragalus (AMNH FARB 30752) in dorsal and anterior views. **I–K,** right calcaneum (AMNH FARB 30753) in medial, lateral, and dorsal views. Abbreviations in appendix 2.

On the lateral third of the dorsal surface of the astragalus lies the articular facet for the calcaneum, which is deeply concave, more so than the articular surface for the tibia. The ventral surface of the astragalus is anteroposteriorly convex and slightly concave mediolaterally.

Calcaneum: The quadrangular calcaneum has four different surfaces (AMNH FARB 30753; fig. 17I–K). The lateral surface shows the outline of a quarter of a circle and is slightly concave. The concave proximal surface receives the distal end of the fibula and is subtrapezoidal, being delimited from the tibial articular surface by a large oblique ridge. The tibial articular surface forms the posteromedial surface of the calcaneum and is smooth and proximodistally concave. Finally, the distal surface of the calcaneum is anteroposteriorly convex and forms the arcuate lateral profile of the element.

Metatarsal III: This element (AMNH FARB 30754 and 30755) is composed of a short and robust shaft that expands proximally and distally (fig. 17C–D). The proximal articular surface is D-shaped, with the dorsomedial corner of the "D" outline projected medially relative to the ventral margin. The proximal half of the medial surface of the bone shows an extensive but shallow triangular depression for articulation with metatarsal II. The ventral surface of metatarsal III bears a large and thick ridge that extends along the proximal two-thirds of the bone. The distal region of the shaft is dorsoventrally compressed, just proximal to the medioventrally expanded distal articular end. The distal surface is dorsoventrally convex and mediolaterally concave, and displays a subrectangular profile. The lateral and medial surfaces of the distal end of metatarsal III are slightly concave (particularly the medial one) and subcircular.

Metatarsal IV: This element (AMNH FARB 30756 and 30757) is relatively more slender than metatarsal III and, with the exception of the proximal and distal ends, its shaft is dorsoventrally compressed (fig. 17E–F). The long axis of the bone is deflected laterodistally. The proximal articular surface is concave and D-shaped, with equally wide dorsal and ventral margins. The ventral surface of the bone is slightly concave throughout its length. The medial surface bears a large tuberosity just proximal to the midlength of the metatarsal. The distal end is nearly equally expanded dorsoventrally and mediolaterally. Its articular surface is dorsoventrally convex and gently concave mediolaterally (less so than in metatarsal III). The lateral and medial surfaces of the distal end of metatarsal IV are oval and deeply concave. The ventral extensor groove is wide and shallow, but slightly more pronounced than in metatarsal III.

Pedal Phalanges: Phalanges II-1 through IV-1 are robust and proximodistally short (fig. 18A–C). These elements show triangular and concave proximal surfaces, with mediolaterally convex dorsomedial and dorsolateral sides, respectively. Phalanx II-1 (AMNH FARB 30758–30760) is the deepest of the three proximalmost phalanges. Phalanx III-1 (AMNH FARB 30761 and 30762) is dorsoventrally compressed and has a subelliptical proximal articular surface. In these three phalanges the distal surfaces are dorsoventrally convex but gently concave mediolaterally.

Pedal phalanx II-2 (AMNH FARB 30765) is a compact bone, twice as wide mediolaterally as it is thick proximodistally (fig. 18D). The proximal surface is smooth and gently concave, with a subtriangular outline that is slightly skewed medially. The ventral margin of the proximal surface is further extended posteriorly relative to the dorsal margin. The restricted dorsal, lateral, and medial surfaces are proximodistally and mediolaterally concave. The distal surface is

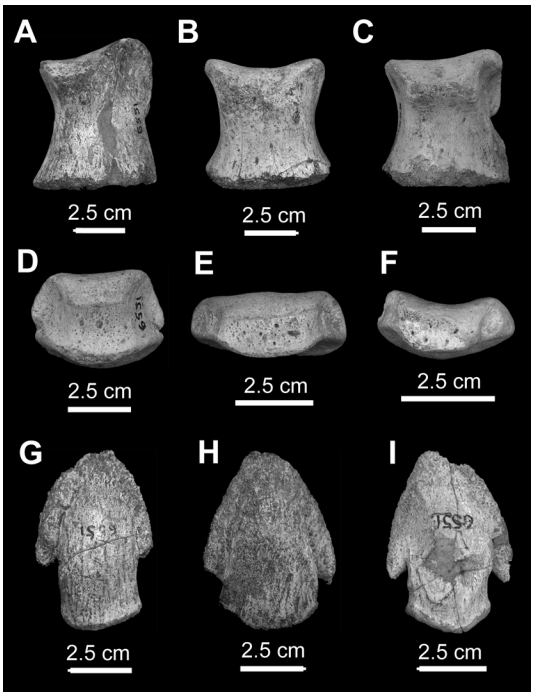

FIGURE 18. Dorsal views of various pedal phalanges of *Gilmoreosaurus mongoliensis*. **A,** left pedal phalanx II-1 (AMNH FARB 30758). **B,** left pedal phalanx III-1 (AMNH FARB 30762). **C,** right pedal phalanx IV-1 (AMNH FARB 30764). **D,** Left pedal phalanx II-2 (AMNH FARB 30765). **E–F,** right (AMNH FARB 30766) and left (AMNH FARB 30767) distal pedal phalanges from digit IV. **G,** pedal ungual phalanx from digit II or IV (AMNH FARB 30768). **H–I,** pedal ungual phalanges from digit III (AMNH FARB 30769 and 30770).

saddle shaped, with a very gentle ventral concavity. Two additional distal phalanges belong to digit IV (AMNH FARB 30766 and 30767) (fig. 18E–F). As usual in hadrosauroids (Prieto-Márquez, 2007), these distal phalanges are at least twice as proximodistally compressed as phalanx II-2. Their distal and proximal surfaces are similar to those of phalanx II-2, but differ in being more mediolaterally concave (fig. 18E).

Unguals (AMNH FARB 30768–30773) are dorsoventrally compressed and proximodistally convex, with elliptical proximal surfaces. These elements are arrow shaped in dorsal and plantar views (fig. 18G–I), unlike the more rounded and proximodistally shortened hooflike contour present in the Hadrosauridae (Horner et al., 2004), but similar to the plesiomorphic morphology seen in non-hadrosaurid iguanodontians such as *Lophorhothon atopus* (e.g., FMNH P27383) and *Probactrosaurus gobiensis* (Norman, 2002: fig. 33). The unguals of digits II and IV are slightly aymmetrical, with more developed medial and lateral flanges, and longer proximal regions (fig. 18G).

DISCUSSION AND CONCLUSIONS

Taxonomic Status and Diagnostic Characters

Brett-Surman (1975) diagnosed *Gilmoreosaurus* on the basis of a supraacetabular process smaller than in any other genus except *Bactrosaurus*; postacetabular process shorter and more dorsomedially deflected than in any other genus; ventrally deflected preacetabular process; slight curvature of the ischial shaft; large rounded knoblike process at the distal end of the

ischium; ischial shaft thicker than in any hadrosaurine; scapula and pubis of "typical hadrosaurine form"; clawed unguals; and maxilla of "typical hadrosaurine form" with smaller tooth count than other genera of the same size.

Except for the shape and relatively reduced dimensions of the postacetabular process of the ilium, these characters do not distinguish *Gilmoreosaurus mongoliensis* from other hadrosauroids. Thus, the size of the supraacetabular process includes its anteroposterior length and lateroventral projection. Being as long as about 75% the length of the iliac central plate, the supraacetabular process of *G. mongoliensis* (e.g., AMNH FARB 30735) is as long as that of some hadrosaurids, such as *Gryposaurus notabilis* (e.g., ROM 764), *G. latidens* (e.g., AMNH FARB 5465), and *Secernosaurus koerneri* (e.g., MACN RN2). As for the lateroventral expansion, the supraacetabular process of *G. mongoliensis* is as expanded as in *Bactrosaurus johnsoni* (Godefroit et al., 1998). Curved ischiac shafts are not uncommon among hadrosauroids (e.g., *Hadrosaurus foulkii,* ANSP 10005); however, the shaft of the ischium is too susceptible to postdepositional distortion, and thus, its curvature may not be a reliable character (Prieto-Márquez et al., 2006a). The thickness of the ischiac shaft is not greater than in other taxa: its width/length ratio is approximately 7%, as in non-hadrosaurid hadrosauroids *Probactrosaurus gobiensis* and *Eolambia caroljonesa,* and the hadrosaurid *Lambeosaurus lambei* (Prieto-Márquez, 2008: fig. I48). In addition, there are taxa with thicker shafts, such as *Hypacrosaurus altispinus* (e.g., CMN 8501) and *Parasaurolophus cyrtocristatus* (e.g., FMNH P27393). The "typical hadrosaurine form" of the maxilla, scapula, and pubis is an ambiguously defined character. Regardless, the maxilla and scapulae of *G. mongoliensis* show several characters (see description above) that are typically present in non-hadrosaurid hadrosauroids and are plesiomorphic for the Hadrosauridae. Although the most informative region of the pubis, the prepubic process, is incompletely preserved, this element also displays characters that are plesiomorphic for hadrosaurids and are common in basal hadrosauroids (see description). Finally, the low maxillary tooth count, ventral knob at the distal end of the ischial shaft, and claw-shaped unguals are plesiomorphic characters in the context of Hadrosauroidea that are typically present in non-hadrosaurid iguanodontians (Norman, 2004; Prieto-Márquez, 2010).

The phylogenetic analysis and osteological observations reported here support the distinction of *Gilmoreosaurus mongoliensis* from *Bactrosaurus johnsoni.* These two species differ in a number of important cranial and appendicular characters (table 1). Some of these have already been noted in previous studies, such as the position of the dorsal process of the maxilla, the degree of ventral deflection of the dentary, the shape of the prepubic process of the pubis, and dorsal profile of pedal ungual phalanges (Gilmore, 1933; Weishampel and Horner, 1986; Godefroit et al., 1998). According to Godefroit et al. (1998), the posterior process of the jugal of *B. johnsoni* is narrower than in *G. mongoliensis.* However, this process is not preserved in the latter (fig. 2). These authors also consider that preacetabular process of the ilium of *B. johnsoni* is more deflected ventrally than in *G. mongoliensis.* However, in both taxa the process forms 140°–146° angles with the plane containing the acetabular margin. Two other characters used by Godefroit et al. (1998) to distinguish *B. johnsoni* from *G. mongoliensis* were the thickness and distal process of the ischiac shaft, which they considered greater in the former species. However, the shafts of both taxa have a width/length ratio of 7%–8% (Prieto-Márquez, 2008:

TABLE 1. Characters distinguishing *Gilmoreosaurus mongoliensis* from *Bactrosaurus johnsoni*.

Character	*Gilmoreosaurus mongoliensis*	*Bactrosaurus johnsoni*
Maxilla, position of base of dorsal process	At midlength of maxilla	Posterior to midlength of maxilla
Maxilla, orientation of ectopterygoid ridge	19°	25°–32°
Maxillary teeth, secondary ridges	Absent	Present
Dentary, ventral deflection relative to tooth row	10°	24°
Ilium, ischial tuberosity	Present	Absent
Ischium, thumblike posterodorsal extension of iliac peduncle	Large	Small
Pubis, proximal constriction of prepubic process	As long as distal blade	Shorter than distal blade
Pubis, distal blade of prepubic process	Shallow, not deeper than width of acetabular margin	Deeper than width of acetabular margin
Pedal ungual phalanges	Pointed and narrow anterior margin	Rounded and broad anterior margin

fig. I48). Comparison of the distal process of *G. mongoliensis* (e.g., AMNH FARB 30739) with that of *B. johnsoni* (e.g., SBDE 95E5/26) showed no substantial difference in size (considering also that the ventral end of the distal process of AMNH FARB 30739 is eroded).

Phylogenetic Inference

A parsimony analysis resulted in nine equally most parsimonious trees of 839 steps each (CI = 0.54, RI = 0.79, 34.4% missing data) found in 979 of the 10,000 replicates. *Gilmoreosaurus mongoliensis* was inferred to be a non-hadrosaurid hadrosauroid, as the sister taxon to the clade composed of all hadrosauroids closer to *Telmatosaurus transsylvanicus* than to *Bactrosaurus johnsoni* (fig. 19). This phylogenetic position of *G. mongoliensis* was supported by three unambiguous synapomorphies (hereinafter, numbers outside and inside square brackets indicate characters and character states, respectively, corresponding to the data set of Prieto-Márquez, 2010): reduced medial projection of the symphyseal process of the dentary (38[0]); base of the maxillary dorsal process centered around the midlength of the maxilla (90[2]); and presence of ischial tuberosity, so that the ischial peduncle of the ilium is composed of two protrusions of similar size (242[2]). Additionally, *Gilmoreosaurus mongoliensis* showed two hadrosauroid unambiguous synapomorphies: ventral deflection of the dentary originating between two-thirds and 78% of the length of the dental battery (37[1]) and ilium with a ratio between the dorsoventral depth of the central plate and the distance between the pubic peduncle and the caudodorsal prominence of the ischial peduncle of 0.8 or greater (234[0]).

Exclusion of *Gilmoreosaurus mongoliensis* from the Hadrosauridae resulted from lack of the following synapomorphies: ilium with ventralmost margin of the supraacetabular process located anterodorsally relative to ischial tuberosity of the ilium (235[1]); anteroposterior length

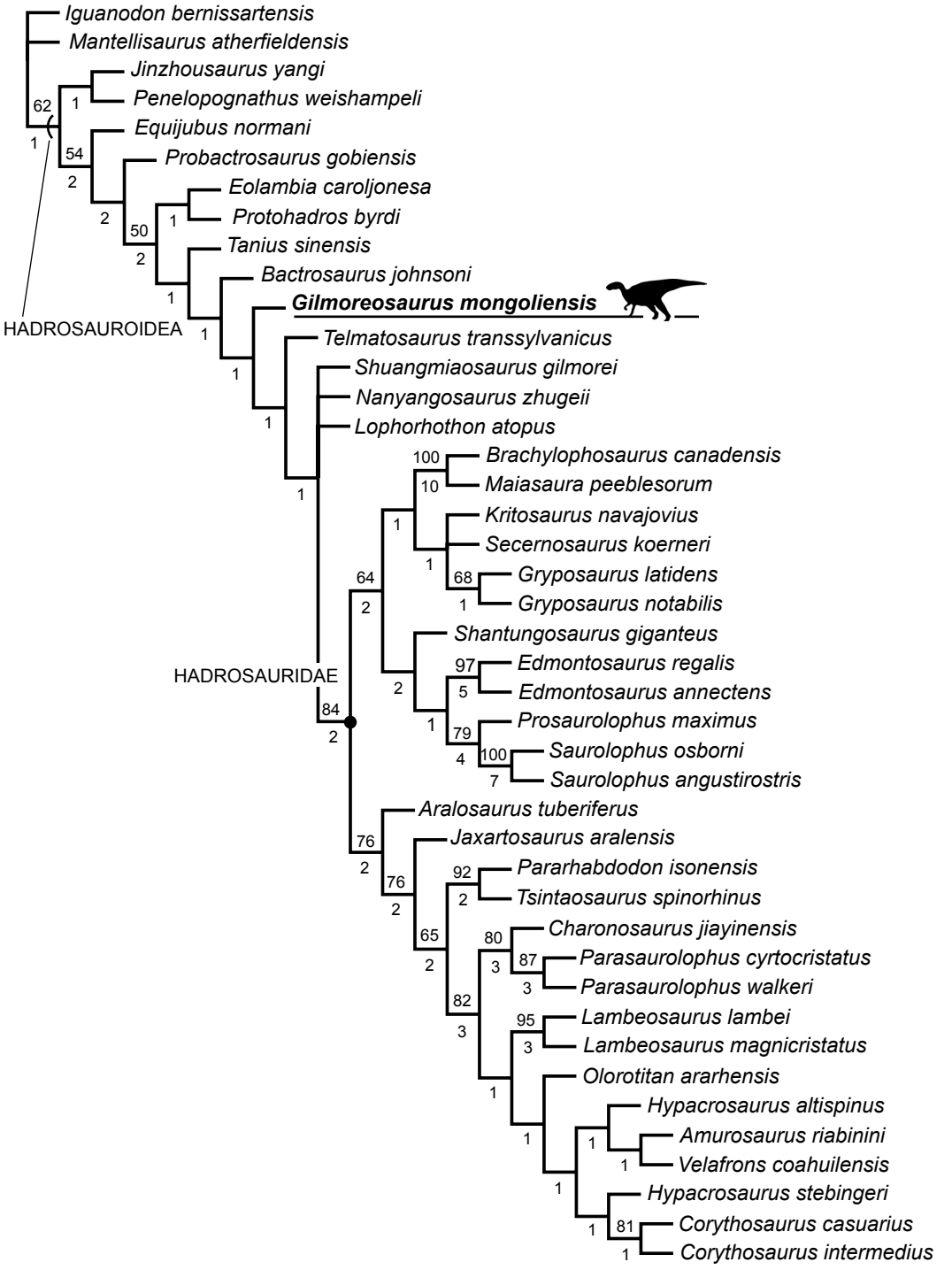

FIGURE 19. Strict consensus cladogram of the nine most parsimonious trees resulting from maximum parsimony analysis of 41 hadrosauroid species, showing the phylogenetic position of *Gilmoreosaurus mongoliensis*.

of the supraacetabular process of the ilium being less than 55% the length of the iliac central plate (237[3]); absence of ridge on the lateral surface of the acetabular margin of the pubis (257[1]); relatively elevated lateral surface of the anterodorsal region of the maxilla (89[1]); medial orientation of the articular surface of the rostral process of the jugal, which is bounded only caudally by a rim of bone (107[1]); absent or poorly developed squamosal buttress of the quadrate (120[0]); angle between the scapular and glenoid facets of the coracoid up to 115° (207[1]); strongly concave anteromedial margin of the coracoid (208[1]); long (209[1]) and recurved ventral process of the coracoid (210[1]); arcuate dorsal margin of the scapula (211[1]); and mediolaterally broad and proximodistally shortened pedal unguals (285[1]).

ACKNOWLEDGMENTS

We thank P. Barrett, B. Battail, M. Brett-Surman, D. Brinkman, K. Carpenter, S. Chapman, J. Cheng, L. Chiappe, Z. Csiki, R. Culbertson, T. Culver, P. Currie, T. Daeschler, R. Dante, C. Delgado, J. Desojo, B. Espinosa, D. Evans, Z. Fang, M. Feuerback, R. Gaete, A. Galobart, E. García, J. Gardner, T. Gates, M. Getty, P. Godefroit, M. del R. Gómez, M. Goodwin, D. Goujet, D. Grigorescu, A. Heckert, A. Henrici, R. Hernández, P. Holroyd, J. Horner, B. Iwama, B. Jacobs, L. Jacobs, Y. Jun, J. Kobalynski, A. Kramarz, M. Lamanna, J. Lamb, W. Langston, T. Lehman, C. de León, L. Liping, J. Li-Young, S. Lucas, E. Lund, K. Madalena, S. Maganuco, P. Makovicky, B. McLeod, M. Montellano, I. Morrison, C. Muñoz, L. Murray, H. Osmolska, P. Owen, J. Padilla, J. Peel, M. del C. Perrillat, M. Pierce, G. Plodowski, Z. Qin, R. Reisz, L. Rinehart, T. Rowe, K. Sabath, G. Salinas, C. Dal Sasso, C. Serrano, K. Seymour, K. Shepherd, W. Simpson, E. Steurbaut, S. Stuenes, Li Tao, P. Taquet, D. Vineyard, O. Vogel, D. Weishampel, C. Weißbrod, D. Winkler, Xu X., L. Zanno, R. Zapata, K. Zhang, L. Zhong, and R. Zúñiga for access to specimens under their care. Thanks to C. Mehling for his work on recataloging the specimens of *Gilmoreosaurus mongoliensis.* Funds for this study were provided by a Kalbfleisch Research Fellowship from the American Museum of Natural History, the Charlotte and Walter Kohler Charitable Trust, the National Science Foundation (EAR 0207744 and DBI 0446224 grants presented to G. Erickson), and the Ministry of Education and Science of Spain (CGL2005-07878-C02-01 grant presented to A. Galobart).

REFERENCES

Beneden, P. 1881. Sur l'arc pelvien chez les dinosauriens de Bernissart. Bulletin de l'Academie Royale des Sciences, des Lettres et des Beaux-arts de Belgique, 3 série 1: 600–608.

Berkey, C.P., and F.K. Morris. 1927. Geology of Mongolia. Natural history of Central Asia, vol. 1. New York: American Musuem of Natural History, 475 pp.

Bremer, K. 1988. The limits of amino acid sequence data in angiosperm phylogenetic reconstruction. Evolution 42: 795–803.

Brett-Surman, M.K. 1975. The appendicular anatomy of hadrosaurian dinosaurs. M.Sci. thesis, University of California, Berkeley, 101 pp.

Brett-Surman, M.K. 1979. Phylogeny and paleobiogeography of hadrosaurian dinosaurs. Nature 277: 560–562.

Brett-Surman, M.K. 1989. A revision of the Hadrosauridae (Dinosauria: Ornithischia) and their evolution during the Campanian and Maastrichtian. Ph.D. dissertation, George Washington University, Washington, DC., 272 pp.

Brett-Surman, M.K., and J.R. Wagner. 2007. Discussion of character analysis of the appendicular anatomy in Campanian and Maastrichtian North American hadrosaurids—variation and ontogeny. *In* K. Carpenter (editor), Horns and beaks. Ceratopsian and ornithopod dinosaurs: 135–169. Bloomington: Indiana University Press.

Carpenter, K., D. Dilkes, and D.B. Weishampel. 1995. The dinosaurs of the Niobrara Chalk Formation (Upper Cretaceous, Kansas). Journal of Vertebrate Paleontology 15: 275–297.

Chen, P. 1983. A survey of the non-marine Cretaceous of China. Cretaceous Research 4: 123–143.

Cope, E.D. 1870. Synopsis of the extinct Batrachia, Reptilia and Aves of North America. Transactions of the American Philosophical Society 14: 1–252.

Currie, P.J., and D.A. Eberth. 1993. Paleontology, sedimentology and paleoecology of the Iren Dabasu Formation (Upper Cretaceous), Inner Mongolia, People's Republic of China. Cretaceous Research 14: 127–144.

Dollo, L. 1888. Iguanodontidae et Camptonotidae. Comptes Rendus Hebdomadaires des Séances de l'Académie des Sciences 106: 775–777.

Donoghue, M.J., R.G. Olmstead, J.F. Smith, and J.D. Palmer. 1992. Phylogenetic relationships of Dipsacales based on rbcL sequences. Annals of the Missouri Botanical Garden 79: 672–685.

Felsenstein, J. 1985. Confidence limits on phylogenies: an approach using the bootstrap. Evolution 39: 783–791.

Gates, T.A., and S.D. Sampson. 2007. A new species of *Gryposaurus* (Dinosauria: Hadrosauridae) from the late Campanian Kaiparowits Formation, southern Utah, USA. Zoological Journal of the Linnean Society 151: 351–376.

Gilmore, C.W. 1933. On the dinosaurian fauna of the Iren Dabasu Formation. Bulletin of the American Museum of Natural History 67 (2): 23–78.

Godefroit, P., Z.-M. Dong, P. Bultynck, H. Li, and L. Feng. 1998. Sino-Belgian Cooperative Program. Cretaceous Dinosaurs and Mammals from Inner Mongolia: 1) New *Bactrosaurus* (Dinosauria: Hadrosauroidea) material from Iren Dabasu (Inner Mongolia, P.R. China). Bulletin de l'Institute Royal des Sciences Naturelles du Belgique 68: 1–70.

Godefroit, P., S. Zan, and L. Jin. 2001. The Maastrichtian (Late Cretaceous) lambeosaurine dinosaur *Charonosaurus jiayinensis* from north-eastern China. Bulletin de l'Institut Royal des Sciences Naturelles de Belgique 71: 119–168.

Godefroit, P., H. Li, and C.-Y. Shang. 2005. A new primitive hadrosauroid dinosaur from the Early Cretaceous of Inner Mongolia (P. R. China). Comptes Rendus Palevol 4: 697–705.

Goloboff, P.A., J.S. Farris, and K. Nixon. 2008. TNT, a free program for phylogenetic analysis. Cladistics 24: 774–786.

Granger, W., and C.P. Berkey. 1922. Discovery of Cretaceous and older Tertiary strata in Mongolia. American Museum Novitates 42: 1–7.

Head, J.J. 1998. A new species of basal hadrosaurid (Dinosauria, Ornithischia) from the Cenomanian of Texas. Journal of Vertebrate Paleontology 18: 718–738.

Horner, J.R., D.B. Weishampel, and C.A. Forster. 2004. Hadrosauridae. *In* D.B. Weishampel, P. Dodson, and H. Osmólska (editors), The Dinosauria. 2nd ed.: 438–463. Berkeley: University of California Press.

International Commission on Zoological Nomenclature. 1999. International Code of Zoological Nomenclature. 4th ed. London: International Trust for Zoological Nomenclature, 305 pp.

Jerzykiewicz, T., and D.A. Russell. 1991. Late Mesozoic stratigraphy and vertebrates of the Gobi Basin. Cretaceous Research 12: 345–377.

Kirkland, J.I. 1998. A new hadrosaurid from the Upper Cretaceous Cedar Mountain Formation (Albian-Cenomanian: Cretaceous) of eastern Utah—the oldest known hadrosaurid (Lambeosaurinae?). New Mexico Museum of Natural History and Science Bulletin 14: 283–295.

Leidy, J. 1858. *Hadrosaurus foulkii,* a new saurian from the Cretaceous of New Jersey, related to *Iguanodon.* Proceedings of the Academy of Natural Sciences of Philadelphia 10: 213–218.

Liu, J., and X. Wu. 1990. Cretaceous-Tertiary charophyte fossils in northern Xinjiang. *In* Institute of Geology, Chinese Academy of Geological Sciences; Geological Brigade of Northwestern Petroleum Geological Bureau, Ministry of Geology and Mineral Resources; Academy of Prospecting and Developing Xinjiang Bureau of Petroleum (editors), Study on the micropaleobotany from the Cretaceous-Tertiary of the oil-bearing basins in some regions of Qinghai and Xinjiang: 181–229. Beijing: China Environment Science Press.

Lull, R.S., and N.E. Wright. 1942. Hadrosaurian dinosaurs of North America. Geological Society of America Special Papers 40: 1–242.

Lund, E.K., and T.A. Gates. 2006. A historical and biogeographical examination of hadrosaurian dinosaurs. New Mexico Museum of Natural History and Science Bulletin 35: 263–276.

Maddison, D.R., and W.P. Maddison. 2003. MacClade version 4.0. Sunderland, MA: Sinauer Associates.

Marsh, O.C. 1881. Principal characters of American Jurassic dinosaurs. Pt. IV. American Journal of Science (ser. 3) 21: 417–423.

Maryanska, T., and H. Osmólska. 1981. Cranial anatomy of *Saurolophus angustirostris* with comments on the Asian Hadrosauridae (Dinosauria). Palaeontologia Polonica 42: 5–24.

Norman, D.B. 2002. On Asian ornithopods (Dinosauria: Ornithischia). 4. *Probactrosaurus* Rozhdestvensky, 1966. Zoological Journal of the Linnean Society 136: 113–144.

Norman, D.B. 2004. Basal Iguanodontia. *In* D.B. Weishampel, P. Dodson, and H. Osmólska (editors), The Dinosauria, 2nd ed.: 413–437. Berkeley: University of California Press.

Owen, R. 1842. Report on British fossil reptiles. Part II. Report of the eleventh meeting of the British Association for the Advancement of Science, July 1841: 66–204.

Parks, W.A. 1920. The osteology of the trachodont dinosaur *Kritosaurus incurvimanus.* University of Toronto Studies, Geological Series 11: 1–74.

Prieto-Márquez, A. 2007. Postcranial osteology of the hadrosaurid dinosaur *Brachylophosaurus canadensis* from the Late Cretaceous of Montana. *In* K. Carpenter (editor), Horns and beaks. Ceratopsian and ornithopod dinosaurs: 91–115. Bloomington: Indiana University Press.

Prieto-Márquez, A. 2008. Phylogeny and historical biogeography of hadrosaurid dinosaurs. Ph.D. dissertation, Florida State University, 936 pp.

Prieto-Márquez, A. 2010. Global phylogeny of Hadrosauridae (Dinosauria: Ornithopoda) using parsimony and Bayesian methods. Zoological Journal of the Linnean Society 159: 435–502.

Prieto-Márquez, A., and J.R. Wagner. 2009. *Pararhabdodon isonensis* and *Tsintaosaurus spinorhinus*: a new clade of lambeosaurine hadrosaurids from Eurasia. Cretaceous Research 30: 1238–1246.

Prieto-Márquez, A., D.B. Weishampel, and J.R. Horner. 2006a. The dinosaur *Hadrosaurus foulkii* from the Campanian of the East Coast of North America, with a reevaluation of the genus. Acta Palaeontologica Polonica 51: 77–98.

Prieto-Márquez, A., R. Gaete, G. Ribas, A. Galobart, and M. Boada. 2006b. Hadrosauroid dinosaurs from Western Europe: *Pararhabdodon isonensis* and *Koutalisaurus kohlerorum* n. gen. et sp. Journal of Vertebrate Paleontology 26: 929–943.

Riabinin, A.N. 1930. [*Mandchurosaurus amurensis,* nov. gen., nov. sp., a hadrosaurian dinosaur from the Upper Cretaceous of Amur River]. Mémoires de la Societé Paléontologique de Russie 59: 1–36. [in Russian]

Rozhdestvensky, A.K. 1966. New iguanodonts from Central Asia: phylogenetic and taxonomic relationships between late Iguanodontidae and early Hadrosauridae. Paleontological Journal 1966: 103–116.

Rozhdestvensky, A.K. 1977. The study of dinosaurs in Asia. Journal of the Palaeontological Society of India 20: 102–119.

Seeley, H.G. 1888. On the classification of the fossil animals commonly named Dinosauria. Proceedings of the Royal Society of London 43: 165–171.

Steel, R. 1969. Ornithischia. *In* O. Kuhn (editor), Handbuch der Paläoherpetologie: 1–84. Stuttgart: Gustav Fischer.

Swofford, D.L. 2002. PAUP*. Phylogenetic Analysis Using Parsimony (*and Other Methods). Version 4.0b10. Sunderland, MA: Sinauer Associates.

Swofford, D.L., G.J. Olsen, P.J. Waddell, and D.M. Hillis. 1996. Phylogenetic inference. *In* D.M. Hillis, C. Moritz, and B. Mable (editors), Molecular systematics. 2nd ed.: 407–514. Sunderland, MA: Sinauer Associates.

Taquet, P. 1976. [Geology and paleontology of the Gadoufaoua fossil locality. Aptian of Niger]. Cahiers de Paleontologie. Paris: Centre National de la Recherche Scientifique, 191 pp. [in French]

Van Itterbeek, J.V., D.J. Horne, P. Bultynck, and N. Vandenberghe. 2005. Stratigraphy and palaeonvironment of the dinosaur-bearing Upper Cretaceous Iren Dabasu Formation, Inner Mongolia, People's Republic of China. Cretaceous Research 26: 699–725.

Wagner, J.R. 2001. The hadrosaurian dinosaurs (Ornithischia: Hadrosauria) of Big Bend National Park, Bewster County, Texas, with implications for Late Cretaceous Paleozoogeography. M. Sci. thesis, Texas Tech University, Austin, 417 pp.

Wang, X., and X. Xu. 2001. A new iguanodontid (*Jinzhousaurus yangi* gen. et sp. nov.) from the Yixian Formation of western Liaoning, China. Chinese Science Bulletin 46: 1669–1672.

Weishampel, D.B., and J.R. Horner. 1986. The hadrosaurid dinosaurs of the Iren Dabasu Formation (People's Republic of China, Late Cretaceous). Journal of Vertebrate Paleontology 6: 38–45.

Weishampel, D.B., and J.R. Horner. 1990. Hadrosauridae. *In* D.B. Weishampel, P. Dodson, and H. Osmólska (editors), The Dinosauria. 2nd ed.: 534–561. Berkeley: University of California Press.

Weishampel, D.B., D.B. Norman, and D. Grigorescu. 1993. *Telmatosaurus transsylvanicus* from the Late Cretaceous of Romania: the most basal hadrosaurid dinosaur. Journal of Paleontology 36: 361–385.

You, H.-L., L. Zhe-xi, N.H. Shubin, L.M. Witmer, T. Zhi-lu, and T. Feng. 2003a. The earliest-known duck-billed dinosaur from deposits of late Early Cretaceous age in northwestern China and hadrosaur evolution. Cretaceous Research 24: 347–355.

You, H.-L., Q. Ji, J. Li, and Y. Li. 2003b. A new hadrosauroid dinosaur from the Mid-Cretaceous of Liaoning, China. Acta Geologica Sinica 77: 148–154.

Young, C.C. 1958. The dinosaurian remains of Laiyang, Shantung. Palaeontologia Sinica, New Series C 16: 53–138.

Xu, X., X.-J. Zhao, J.-C. Lü, W.-B. Huang, Z.-Y. Li, and Z.-M. Dong. 2000. A new iguanodontian from Sangping Formation of Neixiang, Henan and its stratigraphical implication. Vertebrata PalAsiatica 38: 176–191.

APPENDIX 1

Institutional Abbreviations

AMNH FARB	American Museum of Natural History (Fossil Amphibian, Reptile, and Bird collection), New York, USA
AUMP	University of Alabama Museum of Paleontology, Auburn, USA
CMN	Canadian Museum of Nature, Ottawa, Canada
CPC	Colección Paleontológica de Coahuila, Saltillo, Mexico
CUST	Changchun University of Science and Technology, Changchun, China
FMNH	The Field Museum, Chicago, USA
IRSNB	Institut Royal des Sciences Naturelles de Belgique, Brussels, Belgium
IVPP	Institute of Vertebrate Paleontology and Paleoanthropology, Beijing, China
MACN	Museo Argentino de Ciencias Naturales "Bernardo Rivadavia," Buenos Aires, Argentina
MOR	Museum of the Rockies, Bozeman, USA
NHM	National History Museum, London, United Kingdom
NMMNH	New Mexico Museum of Natural History and Science, Albuquerque, USA
PIN	Palaeontologiceski Institut, Akademii Nauk, Moscow, Russia
PMU	Uppsala University, Museum of Evolution, Uppsala, Sweden
ROM	Royal Ontario Museum, Toronto, Canada
SBDE	Sino-Belgian Dinosaur Expedition
SMU	Shuler Museum of Paleontology, Southern Methodist University, Dallas, USA
UCMP	University of California Museum of Paleontology, Berkeley, USA

APPENDIX 2

Anatomical Abbreviations

ac	acetabular margin
adpr	anterodorsal process
af	alveolar foramina
aicg	anterior intercondylar groove
alv	alveoli
apr	anterior process
ardt	articulation surface for dentary
arex	articulation facet for exoccipital
arfb	articular surface for fibula
arh	articular head
arj	articulation margin for jugal
arlc	articulation surface for lacrimal
armttII	articular depression for metatarsal II
armttIII	articular depression for metatarsal III
armx	articulation surface for maxilla
arpdt	articulation margin for predentary
arpf	articulation surface for prefrontal
arpmx	articulation margin for premaxilla
arpo	articulation surface for postorbital
arqj	articulation face for quadratojugal
arrd	articular depression for radius
artb	articular surface for tibia
arv	articulation surface for vomer
aspr	ascending process
avpr	anteroventral process
bcs	bicipital sulcus
bct	bicipital tubercle
bs	brevis shelf
cf	coracoid foramen
chsf	choanal shelf
cicg	caudal intercondylar groove
cnc	cnemial crest
cof	coracoid facet
ct	centrum

dars	distal articulation surface
dnt	denticles
dp	dental parapet
dpc	deltopectoral crest
dpr	dorsal process
dsbl	distal blade
dspr	distal process
dtr	deltoid ridge
em	external malleolus
epr	eptopterygoid ridge
eps	eptopterygoid shelf
fh	femoral head
ftr	fourth trochanter
gl	glenoid
glf	glenoid fossa
gtr	greater trochanter
icd	internal condyle
icg	intercondylar groove
ilpd	iliac peduncle
im	internal malleolus
ispd	ischial peduncle
issh	ischial shaft
ist	ischial tuberosity
jpr	jugal process
lcc	lacrimal canal
lcd	lateral condyle
lcf	lacrimal foramen
ltf	lateral flange
ltpr	lateral process
ltr	lesser trochanter
mcd	medial condyle
Mckc	Meckelian canal
Mckg	Meckelian groove
mdf	medial flange
mdr	medial ramus
mr	median primary ridge
mtb	medial tuberosity
na	neural arch
nc	neural canal
ns	neural spine
obm	orbital margin
obpr	obturator process
opr	olecranon process
papr	preacetabular process
pars	proximal articulation surface
paspr	posterior ascending process
pbpd	pubic peduncle
pff	prefrontal flange
plpr	palatine process
pltpr	posterolateral process
pmxg	premaxillary groove
poapr	postacetabular process
pocpr	postcotyloid process
polpr	posterolateral process
popbpr	postpubic process
popr	postorbital process
poz	postzygapophysis
pozpr	postzygapophyseal process
ppbpr	prepubic process
ppl	marginal papillae
prcpr	precotyloid process
prz	prezygapophysis
pspr	pseudoacromion process
ptb	posterior tuberosity
ptf	pterygoid flange
ptpr	pterygoid process
pvf	posteroventral flange
pxcn	proximal constriction
qc	quadrate cotylus
qh	quadrate head
qjn	quadratojugal notch
rcd	radial condyle
rf	rostral foramen
rp	rostral process
sapr	supraacetabular process
sbl	scapular blade
scf	scapular facet
scl	sacral lamina
sqb	squamosal buttress
sym	mandibular symphysis
symp	symphyseal process
th	tooth crowns
tpr	transverse process
ucd	ulnar condyle
vjpr	ventral jugal process
vpr	ventral process
vs	ventral sulcus
wf	wear facet

APPENDIX 3

Character codings of 43 iguanodontian species for the 287 osteological characters. The first 286 characters are those in Prieto-Márquez (2010). Character 287 is new and consists of the presence (1) or absence (0) of precotyloid fossa in the squamosal. Brackets indicate polymorphism, whereas claudators indicate that either one of the character states shown may be present.

Iguanodon bernissartensis
00000000000000000000000000000000100001000010000000000000110000000000000000000000000000
0000000000000000100000?01001001000100000000001101000?000?000?1000000?00010000000?0001?00?
?0010?00????101000000000001010000000000000000000100000010010100000000111000000000000000001
1000000110000000001000001

Mantellisaurus atherfieldensis
00000000000000000000000000000000111000100001000000000000110000000000000000000000000001
0000000000000000100000?01001000000100000000001101000?000?000?1000000?0??10000000?0101?00?
?0010?00????10110000000001000000000000000000000010000001000010000000011100000000000000000
1000000110000000001100001

Shuangmiaosaurus gilmorei
0???????????1?00211?????????????000010011000?00011?????????????????0?0?????????????0?100000100??002
10???
??

Nanyangosaurus zhugeii
??
???00??????
???????????1??0?11??1???1?1???????0??

Eolambia caroljonesa
0110300?1000010?0??01???????????001021011000?0001??00?000?0??000000000000000???00000?0?00????
???10?????00?0?01?0102?000???????0?????????????00?0?0?????11?0?00???000???0?0???0??0?1???0???????????
????????0??????????????????????????????1???000001??1?0?0??0???????????111101011010?????????????

Equijubus normani
01?0000?0000??0??0000001001000?00101?010000?0????0010??0??00000000000000000000010000001?001
??000000??0000000?0000101000010000000000?010???000?000?10?001??0???0???0????100?00??0010?00
????001000?00?000?00?????????????????????????????000000000000??000??0?????????????????????????????????
????1

Jinzhousaurus yangi
0?????????????01?0???00?????0??000?02???10?????????0?0??0??000?0000000000000021100??0???00??01?00
???000000?0020010010??1?000000000?00102???00?200?100??????????????????102?00??001000?????1???0?
100??1

Penelopognathus weishampeli
00?0000?000?01??????????????????01000001100010000??
??
??

Probactrosaurus gobiensis
01111002000011??0?0?00?000001?0?1101101200010001??0?0?????000?000000000000000??0???000????0???0?00???00000?00???0?????????????000??00?000??00?000?10(01)0????????0???0???0?0???0??0?1???0?????0?100001??????0?0010000000000000000011??01?11?000000000000110001000012 01???11101001011000 00?????11000?

Protohadros byrdi
01?01(01)0111001111??10101000??14101012211120001001100010000??1100000000000000?0?0???01 0100101010?1011??00000?0100102010 0?00?00000?1?????????00?0000?????????????????????0101?00??0010 ?00????0???00?0?????????????????????????000???

Bactrosaurus johnsoni
011(12)10022?00110111(01)0100100010100012111012 0(01)0100011011010100100100000000000000?000?0?0100101000010110000000?021000101111000000000001110001100?000010001100011100100 1??100???0??0010?00????1010000?0?00?1?0?102000000100101010100??10?1?12001101011(01)110001000?12 00111111111111021001111 00?0110100

Gilmoreosaurus mongoliensis
0112????????1?01111010?0??00010?0??01001????100011?????????????????????????0000?0???0?01002010 00?111100?0?00?0??0?0?0111100????00?????????????00?????????????????????????0??????00????0?????????????????0???????200000?00010101011{01}??1????12101101012011010 10(01)?????0???111111110110001110 0?0110000

Tanius sinensis
??000?????????????????????0000?000000101??1???0??00011?1?0?01100?000?100011110??1000001001?????????????0????0???000?1?1??2?????????10000000010 0?????????120001010111110100 00?????????????????????1??1????????0

Telmatosaurus transsylvanicus
01?1200?0?11110?11100???????????000000012000000110?11000100?000000000000000???000?0?0100201 0?002111??0??00?0????0001??11?????00??????00?1100?000?10??1110???100?1????1101?00??0?1???0????0?0?0000??01??0?????????

Lophorhothon atopus
???22102110??10??1101??00000??00???000?0?00002????0?????0?00?00????????01111100000000?0???20011100?00001??011???????0??0??00?0???0??0?11010?5??0??1000?1????????001000000001?00000210??10?1?12?02102?1??000101111??1101??110121????0???10100?0110000

Amurosaurus riabinini
112221122?00111121101???????????201221112(12)1001112111111111 00?????????????21????00?1?0011212012?2321??21?1101110111?????120100?1010??11{01}110101211?1102111000110 0?100??1?1????????0??1?????010???101??1?????01211111?1?0100221112??1????12?123120?2??????1110110111 1?102111?2011???1110??01????1

Aralosaurus tuberiferus
??????????????1??110????????????????????????????????????0???????????0?0???????????1?000121201??2021??11????1??01?0??????00000?001??1?0?1??00??00?1?????????????11??????1???????????1?????0?01?0101??

Brachylophosaurus canadensis
12223112 2?001111211(01)120211112211312(012)(012)11121110111211111001002131101000000000011
11000?0101002021111222100011110122 11(01)10112110000100(01)(01)(12)11001100101100020101111
1112001111101(12)00?10??0113010?2??0101100(01)01111101111211211 11(01)1?011011121111211120
12203112100011111121111111110111221 10???1110010110111

Maiasaura peeblesorum
12223112 2?001111211??2021111221120211011211101112111110010021311010000000000111000?0101
00202111122210001111012211010012110001 1000(01)11100210000?100?(12)01011111112001111101100
0?00??0112011?4??0101100001111101 1?1211?111111?01101111111?2111201220311210001111112111 1
1111101112211 0???11100101?0111

Charonosaurus jiayinensis
1123311220??11??????????????????00?11111211001112111 11??100??????????????21????00???0?????????
???????2121101010110??????2??0??101112?1210001?21211112111 00??100?000??1?1????????0??1?????0
101??101??1???1????????1?11010012111???10???120123?20120000111?1?????11101?2111??0?1111111
11?01?1??0

Corythosaurus casuarius
12222112101111112 11??01312111310111(12)(01)11121100111211111111001111000011210 1?214??100?
1?00112121121232110212 1101(01)10111100001201002101011112110101211101111110011000110100 1
(01)1?0?100120??12062101010210110111110112111111110100221012111111112012312012100011111 0
11011111112111120210101111110101101

Corythosaurus intermedius
12222112101111112 11??01312111310111(12)(01)11121100111211111111001111000011210 1?214??100?
1?00112121121232110212 1101(01)10111100001201002101011112110101211101111110011000110100 1
(01)1?0?100120??12062001010210110111 11?11211111111010022101211111111201231201210001111 10
11011111112111120210101111110101101

Hypacrosaurus stebingeri
11232(01)01101111212 1???013121113101012211121100111211111101001111000011210 1?214??100?1?
00112121121232110212 1101110111100001201002101011112110101211101111111(01)0110001101??111
?1?100120??12061101010210 11?1?2?1?11211111110010022101 2???????12012312012100011111011011 1
11021111?01101011 1?1?0001101

Hypacrosaurus altispinus
1123211?2?01111121112?13122113 1?1111(12)1112?100?11211111??10011110000112203?214??100?1?00
11212112123211041211 01(01)10111100001201002101001112110101211101101110001 0(01)01101001(0
1)1?1?100120??12061001010210111111211011211111110010022101211111111201231201211201111101
10111111021111102111011101100 01101

Lambeosaurus lambei
1(12)2(23)2112101111(12)12111101(23)11011(34)10111111112110011121111111100111100001122 11?
213??000?1?0011(12)12112123211021211 01(01)10111100001201001101011112110101211101111110 01
10101101001 11?0?110120??12263001010210110111110112111111100100??1{01}1{12}1111111120123 12
012100011111 01?01111111211112011010111111010111101

Lambeosaurus magnicristatus
1?2?21??????11(12)121111?1(23)1?01131011111??12110?111211111??10011110000112211?213??000?1?0
01121121121232?10212110101011110000120100110101111121?010121??01?111??????1?1101??111?0???01
20??12263101010210?1?11?1??11?????11100100221112111?1111201231201210001117101101111?11211
1120210101111?101??101

Edmontosaurus annectens
232131(01)222001121211?21(01)111?11411(23)100(01)0103(12)10011121111100100213111110000000
00221010?0100012021111232100110010103021101120101000001201110111000?0000202011110111
011121011000?10??0111100????0101100101011001111211211111?01(12)111(01)111111111211231211
21000111111310111101201212 2(01)00???1110010110101

Edmontosaurus regalis
232231022200112121102101117?11411(23)100(01)0103(12)10011121111100100213111110000000000221
010?0100012021111232100110010103021101120101000001201110111000?0000202011110111011011210 1
1000?10??0111100????0101100001011001111211111111?012111111111111112012312112100011111131
01111011012121100???1110010010101

Velafrons coahuilensis
1?2221??????111?211??11212?1131??12111112110011121??????10011110000112?02?214???00?1?00112121
1212121??212110111011011000 12??0??10??11???1??101??1?0111?????????1101??111???????20??12?6??01?
10?101?????????????????????010??211????1????120113120120120111 1????111111?21111201100 0??????01??101

Jaxartosaurus aralensis
??00????????????????????
??????????????1??0??021?1120?1??101210?01?0111?0???001101??????????????????1?????0??1?01?1???????????
??0

Kritosaurus navajovius
1222210?2?00112121 10?001??11021?00120011211001112111110?100????????000000000010010?0002012
02111?232100111010023110101121101000000111020 01?000?100?101011110111001121?01?0???0??0112
010?5??010(01)010011?1???2????????????????????????????????
??????????1

Gryposaurus notabilis
132121012?001111211??00200010410(12)02(12)(01)011211001112111110010011211010000000100010 0
011000201302111023210111101101311020112110100000011102011100 0?10002000111?0111001121001
201?30??0111010?1??0100010011011001111211111001 1?111(12)1(12)1111111111111212112122???111?1
1411111???2011122100???1110010011101

Gryposaurus latidens
1320311110001 11?211?????????????21222011211001112111110010021211??0000000?000100??000020130
211102321??????1?????????????0??0?0?0????20????00????????????????????????1?0???0??0111010?1??0?0?0??
???01?0?1111211111001 1?111(01)1201??1????11?121120122000111111411111?012????????0??????0??????1011

Olorotitan ararhensis
1?222112????1121211??11311111?112111111121100111211111111001111000 01?2?02?2????0?0?1?00111
1211212321??41211010101111???0?20?00??????????1?????2?1??1??11?????????????00?11??????120??120?1?0
10100?0??011?12?1121111111101002210?????????120123120121000 11??1?????111?1?21111201 10?0111??
????????

Parasaurolophus walkeri
122?????????11???111111312?1141010202111121??011121111111100111?0000100004?2????000?1?011111
211?0232?1?31211?1010210100001201002121011212100010212101111?????0?1101??121?1?021220??1
2270?0101121011?11111??121111111100012210011110011120133120120000 11??10110111?102111120
11?1111???1?????00

Parasaurolophus cyrtocristatus
12222112100011?????????????????1????????12???0?11211111??100????????10000??2????0?0?1?0????1????0??
??1?????1?????????????????201002101112212100010212?0111111001?0001101???21?1?021220??12270?0101?
2101??111110???????111101012210011 11????121133120120000111?101101111110200011021111111111101??100

Prosaurolophus maximus
23223101 2?0011212110?00(23)11011411110(01)00103(12)1001112111110010021211010000000000221
010?000(01)012021110232101110011 0(01)300120111010101(01)0011111201 1?000?00002010111101100
0112100?102?20??0112110?5??0101100(01)11?11001111211211111?11111(12)1111111111211(23)2120
122000111111401111201201212211 0???1110010111101

Secernosaurus koerneri
12?2310?2?001111?110????11??????002111112?100?112??1?1??100?????????0??????????000?0?0201302????
2121?????????????????????????010000000????0?11000??000201011110 1?0001121????????0??0??????????0?????0?
1??1?1???111011110011?11????1???1????111121020121131111111401111201201212212 0???111???00?????

Saurolophus osborni
23223101 2?0011212110?0031101041?2100001031100111211111001001121101000100000022100 0?0001
012021110232101110011003001(12)011101000110121211212100011200??1?0111?01?000112100110 2?20
??0113110?3??010110?1111110111?1211211111?01?21{01}01111??111211321211220001 11?11411111
??1101?1???10???1110010011101

Saurolophus angustirostris
2321310?2?001121211??00211010411(12)1000010311001112111110010011211010001000000221000?00
010120211102321011100100030 01(12)011101000110121211212100011200?2010111?0??0001121??1102
?20??0113110?3??010110011111101111121211111?01221001111?111121132121122000111?11411111
??11012112010???111?010011101

Shantungosaurus giganteus
2321311?2?00112??11???02????0???21002?1122100??121??????100????????00000??00???0???0??00120211
1?2?21?????????????????1112010000000?1?11?0211?00?000?200011????????1121???{01}0???0??0?1??00????
0????00?1??0?111011211101001 1?00211111??1????121123121121000111111 3?011111100121221 10???1
1100?000010?

Pararhabdodon isonensis
1???????????111?????????????????10022210?????11121????????0?????????????????????0????0011?311??2321
??1?1
?1????????1???01002{12}11???2????????1???????????????

Tsintaosaurus spinorhinus
112(23)31111000111??11??102120113101002221 02(12)1001112111110010001 31?010??2??0?103??000?1
?100111311??2321??412?10111001(12)1011010?0?000????1?0010000?211?0111111101?0?01100??1??????
????0??12????0101?02011?1111100120101111001002211 12??11?111201230201211101 11?111011111?102
1111101101011111?0101101

Complete lists of all issues of *Novitates* and *Bulletin* are available on the web (http://digitallibrary.amnh.org/dspace). Inquire about ordering printed copies via e-mail from scipubs@amnh.org or via standard mail from:

American Museum of Natural History—Scientific Publications
Central Park West at 79th Street
New York, NY 10024

♾ This paper meets the requirements of ANSI/NISO Z39.48-1992 (permanence of paper).